ADDIS ABABA UNIVERSITY

OFFICE OF RESEARCH AND GRADUATE PROGRAMS

FLUORIDE REMOVAL BY LATERITIC SOIL AND ELECTROCHEMICALLY FORMED $Al(OH)_3$

BY

KEFYALEW GOMORO FEYISSA

JUNE 2003

ADDIS ABABA UNIVERSITY

OFFICE OF RESEARCH AND GRADUATE PROGRAMS

FLUORIDE REMOVAL BY LATERITIC SOILS AND ELECTROCHEMICALLY FORMED $Al(OH)_3$

A Thesis

Presented to the

Office of Research and Graduate Programs

Addis Ababa University

In Partial Fulfillment of the Requirements for the

Degree of Master of Science in Chemistry

By

KEFYALEW GOMORO FEYISSA

June 2003

ADDIS ABABA UNIVERSITY

OFFICE OF RESEARCH AND GRADUATE PROGRAMS

FLUORIDE REMOVAL BY LATERITIC SOILS AND ELECTROCHEMICALLY FORMED $Al(OH)_3$

KEFYALEW GOMORO FEYISSA

Department of Chemistry

Faculty of Science

APPROVED BY EXAMINING BOARD:	**SIGNATURE**
Dr. Bernd Hundhammer	_____
Advisor	
Dr. Negussie Megersa	_____
Advisor	
Dr. Feleke Zewge	_____
Advisor	
Prof. B.S. Chandravanshi	_____
Examiner	
Dr. Tadesse Wondimu	_____
Examiner	

DECLARATION

I, the undersigned, declare that this thesis is my original work and has not been presented for any degree in any other University and all the sources of material used for the thesis have been duly acknowledged.

Name: Kefyalew Gomoro Feyissa

Signature: _____

This thesis has been submitted for examination with our approval as University Advisors.

Name:	Signature:
Dr. Bernd Hundhammer	
Dr. Negussie Megersa	_____
Dr. Feleke Zewge	_____

Date and Place of Submission: Department of Chemistry

Addis Ababa University

June 2003

DEDICATION

To my parents, brothers and sisters

Acknowledgements

I am highly indebted to my research advisors, Dr. Bernd Hundhammer, Dr. Negussie Megersa and Dr. Feleke Zewge, for their dedicated assistance, consistent guidance, invaluable comments, suggestions and constructive criticisms throughout my research work without which this work would not have been realty. They should also be acknowledged for providing me with literatures related to my research work and computer for writing my seminar papers, progress reports and my final thesis. Dr. Bernd Hundhammer deserves additional credit for his usual heartfelt discussion and lecture in the laboratory from which I benefited a lot; beyond words to express.

I would like to thank Dr. Alessandro Rivaldino from University of Caliary, Italy and Dr. Utz Karmar from University of Karlsruhe, Germany for their kind cooperation in carrying out XRD and XRF analysis of our soil samples.

My appreciation also goes to Prof. Jan-Ake Jonsson (Lund University, Sweden), Prof. V.J.T Raju, Obbo Tamesgen Faraja, Obbo Tamane Lamu, Obbo Wakgari Addu, Obbo Ifaa Hussien, Obbo Ahmed Hussien and Obbo Alemayehu Essayas for providing me with books and literatures for my research work.

My thanks also go to Prof. B.S. Chandravanshi for his tireless encouragement, guidance, friendly approach, and willingness for discussion and help whenever I need him; Dr. Merid Tessema and Obbo Kitessa Hundarra for their regular encouragement; Ato Alemayehu Abebaw and Ato Tarekegn Berhanu for encouraging me not give up hope in any challenging and frustrating conditions. This helped me a lot in overcoming all those conditions with extreme patience, which anyone could hardly tolerate. I would also like to acknowledge Ato Sahlemicael Deme and W/o Woinshet Gebeyehu for the technical assistance they rendered me during the course of the study and for all they did for me.

I feel pleasure in thanking Obbo Tuli Gamada, Obbo Dheressa Gamada, Aadde Birane Gomoro, Obbo Qanate Gomoro, Obbo Faqqada Tuli, Obbo Dassalegn Warke and Obbo Dassalegn Fufa for their material and moral

support starting from my elementary school up to this level. It is my pleasure to express my heartfelt gratitude to Jifare Tolera for her love, moral support and utmost encouragement which contributed much to my success.

I also extend my gratitude to all Chemistry Graduate students of my batch for their encouragement, especially to Obbo Mosissa Adi, Obbo Aweke Kebede, Obbo Abdulkadir Shube and Obbo Negash Getachew for their never-ending encouragement and deep concern about my progress in the research work. Ato Mesay Mulugeta and Ato Tewodros Kassa are also acknowledged for their encouragement, usual discussion on our research areas and for their infinite help whenever I face problem on computer.

A special heartfelt word of thanks is also due to Obbo Tadassa Jalata and Obbo Dagim Jirata, my room-mates, for their understanding, patience and passing ups and downs with me during our stay together for two years in a room during our Graduate studies.

Finally, I would like to thank Dilla College of Teacher Education and Health Sciences for sponsoring my education.

FLUORIDE REMOVAL BY LATERITIC SOILS AND ELECTROCHEMICALLY FORMED $Al(OH)_3$

By Kefyalew Gomoro

Advisors: Dr. Bernd Hundhammer, Dr. Negussie Megersa and Dr. Feleke Zewge.

CONTENTS

Page

LIST OF FIGURES

LIST OF TABLES

ABSTRACT

The ability of lateritic soils to remove fluoride from water was studied to clarify some basic issues a) is there a correlation between the mineral composition of the soils and their ability to remove fluoride? b) which processes account for the fluoride removal? c) is the fluoride removal ability increased by a thermal treatment of the soils? and d) which kind of fluoride containing species remain in the soil treated water? The results obtained indicate that fluoride removal and gibbsite content of the soils are correlated. From this it can be concluded that gibbsite is the active component in lateritic soils in the fluoride removal. Speciation analysis reveals that at low free fluoride concentrations the dissolution of gibbsite facilitated by the adsorption of fluoride onto gibbsite accompanied by the formation of aluminum fluoro complexes can explain the mechanism of fluoride removal. The question to which extent the exchange of hydroxide ion with fluoride ion in gibbsite takes place in the defluoridation process cannot be answered with certainty. The electrochemical investigations of aluminum electrodes by cyclic voltammetry, impedance spectroscopy and potentiometry have shown that passivation of the aluminum electrodes is a drawback of the defluoridation of low fluoride solutions by electrochemically generated $Al(OH)_3$ but it might be possible at higher fluoride concentrations.

Key words: Fluoride removal, lateritic soils, speciation analysis, complexed fluoride,

Alzheimer's disease, electrochemical behaviors, passivation, votammogram,

impedance spectroscopy, removal capacity and adsorption isotherm.

1. INTRODUCTION

Water is a basic commodity, which will be needed in ever increasing quantities with increasing urbanization and industrialization in the world. Water is a source of life, a fundamental requirement for health and main need for industrialization; it is mankind's most precious commodity. It is essential for all forms of growth and development - humans, animals and plants. However, independent of the purpose water is used for it has been recognized that its suitability for a specific purpose can be affected by other substances dissolved or suspended in it. Contamination of drinking water by fluoride is one such example [1].

Fluoride is widely distributed in nature and is present in rock minerals, soil, water, plants, foods and even in the atmosphere [2-5]. It enters into human body through a variety of sources like water, food, air, medicine and cosmetics. Among these, drinking water is the most common source which makes fluoride available to human beings [6]. Fluoride illustrates strikingly the classical medical concept that the effect of a substance depends on the dose. Paracelsus (1493-1541) said ″All substances are poisons; there is non that is not a poison. The right dose differentiates a poison and a remedy [7].” Fluoride in drinking water may be either beneficial or detrimental to human health depending on its concentration. Low levels of fluoride are required for humans and other animals and have beneficial effects on tooth and bone structure since it renders tooth enamel relatively immune to bacteriological attack. However, ingestion of excessive fluoride causes skeletal and dental fluorosis [8-13].

The WHO guideline published in 1984 has set a permissible upper limit for fluoride in drinking water to 1.5 mg/l to protect humans from fluorosis. In setting national standard for fluoride, it is particularly important to consider climatic conditions, volume of water intake and intake of fluoride from other sources [14, 15]. Due to these factors, the optimal level of fluoride in drinking water varies from place to place and many countries have established their own guidelines. For example, India has lowered its permissible upper limit from 1.5 ppm to 1.0 ppm in 1998; and in South Africa an optimal range of 0.4 to 0.7 ppm has been recommended [16]. The Ethiopian Ministry of Water Resources has proposed recently a permissible value of 3.0 ppm fluoride in drinking water for Ethiopia [17]. This value seems to be unreasonable if the climatic conditions of Ethiopia in general and the Ethiopian Rift Valley in particular are taken into considerations. In higher temperature areas, like tropical regions, the recommended value should be lower than that of WHO because of the relatively higher water consumption.

Endemic fluorosis is now known to be a global problem, occurring in all continents affecting many people. It is a problem in many developing countries like India, Pakistan, Algeria, Ethiopia, Morocco, Egypt, Tanzania, Far East countries etc. and has been reported sporadically in other parts (Argentina, Canada, USA, Japan, etc.) of the world [9, 18].

Fluoride concentration above 1.5 mg/l has been reported from many parts of Ethiopia (Figure 1), but the highest levels are found in the Rift Valley, the low land area with the highest volcanic activity in the country [19].

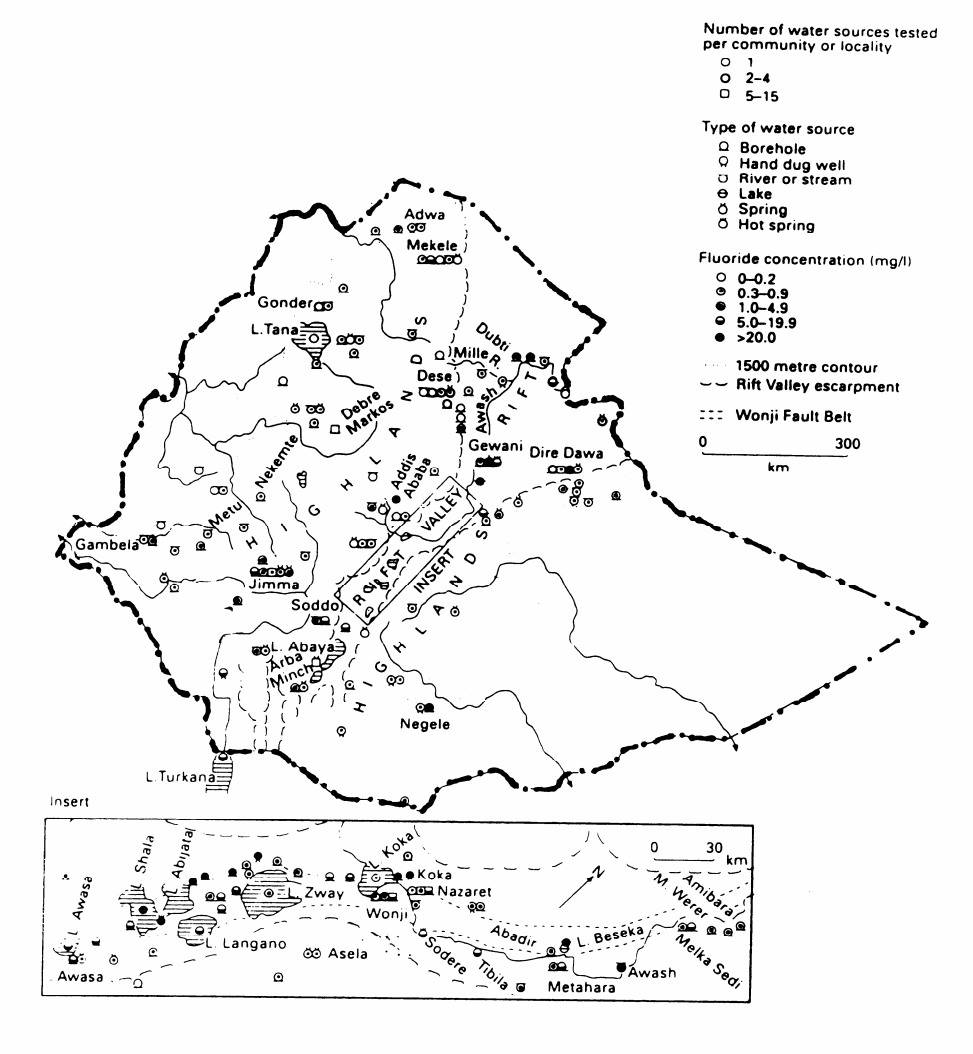

Figure 1. Map showing the distribution of fluoride in Ethiopia.

The fluoride concentrations of waters in the Rift Valley, which are supplied by groundwater and boreholes, were reported to be between 1 and 36 ppm with a mean of 10 ppm [20]. As a result, both dental and skeletal fluorosis are prevalent in this region of the country. Thermal waters in Ethiopian Rift Valley are characterized by high sodium, bicarbonate and fluoride concentrations, and near-neutral to alkaline pH. Gizaw [21] has attributed the high fluoride concentration in the Rift to acid volcanic, high temperature rifting, high subsurface carbon

dioxide pressure and low calcium content (due to removal of calcium by carbonate precipitation). These findings are consistent with the results of Chandra *et al.* [22] and Teoita *et al*. [23] who concluded that water with low hardness, which is low in calcium and magnesium contents and high alkalinity, have high fluoride content and hence present risks of fluorosis.

The public health and economic impact of fluorosis is significant in many endemic areas in view of the occurrence of debilitating skeletal fluorosis in humans and more recent discovery of pathology in cattle, sheep and other livestock [24]. No economic impact studies of fluorosis have been conducted in Ethiopia, but the large number of affected persons and disability of workers with crippling disease indicate that the economic losses are significant. For example, between 1976 and 1984, Wonji-Shoa Farm Estate had retired 530 workers due to disability, 46% of them with a radiological diagnosis of skeletal fluorosis. Another 300 workers were subsequently examined after complaints of pains and aches in the joints and limitation of movements. Sixty five percent of them were diagnosed with skeletal fluorosis, 30 persons presenting with the severe crippling form characterized by complete physical incapacity, cervical myelopathy, radioculomyelopathy and dorso-lumbar radiomyelopathy [20].

Fluorosis not only affects the body of persons but also renders them socially and culturally crippled [25]. It is a disease for which no medical treatment exists. Fluoride poisoning (fluorosis) can be prevented or minimized by using alternative water sources (like surface water, low-fluoride ground water and rain water), increasing the nutritional status of the population at risk (adequate intake of calcium reduces the risk of dental fluorosis during the childhood) and by removing excessive fluoride from drinking water. From experience,

defluoridation of drinking water appears to be a simpler practical solution to prevent the adverse effects of fluoride. As a result, several methods of water defluoridation have been suggested and practiced to alleviate or minimize the problem of fluorosis. Different defluoridation methods with their pros and cons were discussed in different theses [26, 27] and they may be grouped into three general categories:

i) Precipitation methods which involve the addition of chemicals and the formation of fluoride precipitates or coprecipitates. Nalgonda technique which involves a direct addition of alum and lime depending on the fluoride content of water is a commonly used technique in this respect [28]. Aluminum sulphate [29], aluminum hydroxide [30], magnesium hydroxide [29] and sodium aluminate [29] can also be used as a fluoride coagulant. The major problems associated with the use of precipitation methods include the requirement of large amount of chemicals, production of large amount of sludge, the need for adjusting pH before and after treatment and ineffectiveness with water sources having high amount of dissolved solid.

Among the precipitation methods, defluoridation by electrochemical method is briefly discussed below. The electrolytic defluoridation is based on the dissolution of aluminum anode and subsequent formation of cryolite or aluminum hydroxide and other aluminum complexes [31, 32]. The formation of cryolite may be favored under low pH, where aluminum ion is most stable, and high fluoride concentration near the anode. The movement of fluoride ions under the influence of electric field facilitates this process. The electrochemical method is advantageous in that there is no need of adding chemicals, produces low volume of sludge, operator friendly, and can be used for removal of both toxic organic and inorganic chemicals [1, 32, 33]. Electrochemical techniques are becoming increasingly attractive in dealing with environmental problems as the electrons provide clean, versatile and efficient reagents for

many redox processes [33]. However, the electrochemical behaviors of aluminum has not yet been studied and documented.

The major problems of the electrochemical method are cost and availability of electrical energy, possible existence of aluminum in the treated water and passivation of the anode [31, 32]. Possibilities such as the use of solar energy has to be evaluated in order to test the applicability of the method and considering the advantages the overall cost of the system has to be evaluated.

ii) Membrane methods currently available on commercial scale for fluoride removal are reverse osmosis and electro dialysis. Reverse osmosis utilizes a semi-permeable membrane which removes total dissolved solids by applying pressure exceeding the osmotic pressure of the solution. In electro dialysis, anion selective and cation selective membranes are placed in alternate layers and electric field is applied to move the ions in water through these membranes [34]. The shortcomings of these methods are that they are not selective only to fluoride and remove all or part of the dissolved ions present in the raw water, produce concentrated brine which must be disposed of properly to prevent pollution and are relatively energy intensive and consequently expensive to operate. Membrane fouling by colloidal material and certain dissolved salts is also another problem associated with these methods [35, 36].

iii) Adsorption methods involve removal of fluoride due to physical, chemical, or ion exchange interactions with the adsorbent. In these methods, the saturated adsorbent can be regenerated by backwashing with a mild acid or alkali [37-40]. The effluent from backwashing is rich in the accumulated fluoride and therefore must be disposed of carefully to

avoid contaminating nearby surface and ground waters. Zeolites [37], bone char [38], activated alumina [39, 40], alum sludge [18] and soils [10, 26, 35, 41, 42] are some of the adsorbents used in adsorption methods. Defluoridation by soils is briefly discussed below:

Although there are established defluoridation methods, their application in the remote rural areas of the Ethiopian Rift Valley is limited because they require at least an analytical monitoring of the fluoride content in the water. High cost of operation and maintenance and the requirement of trained personnel are other serious drawbacks for the utilization of those methods in rural areas. Exploiting the ability of soils to adsorb cations and anions as well seems a promising approach to solve the problem and has attracted the interest of many research groups [10, 26, 35, 41, 42]. Different soil samples were collected from different parts of Ethiopia and were tested for their defluoridating capacities. The results show that soils can be used as alternatives for defluoridation purposes and the defluoridating capacities of the soil samples vary over a wide range [26]. The different affinities of the soil samples for the fluoride ions may be due to the difference in their mineral compositions. Moges *et al.* [41] investigated the defluoridation of water by chips of clay pot and bricks. The investigation has shown that 120 g of each ground clay pot and brick removed 90% of fluoride from 1 L of water containing 10 ppm F^- in a contact time of 180 h while raw clay soil (not fired) showed a capacity of 72% under the same experimental conditions. This result indicates that firing is an important requirement to achieve better defluoridation. The same study indicated that the capacity of raw clay soils is low as compared to materials such as activated alumina [39, 40]. Zevenbergen *et al.* [10] have also investigated the fluoride removal capacity of Ando soils in Kenya. According to this study, the defluoridating capacity of the soil is 5.5 mg/g. This value is higher compared to the capacity of ground clay and ground brick (0.2 mg/g) investigated by Moges *et al.* [41]. Another recent study on lateritic soils showed that the soils have certain

ability to adsorb fluoride from aqueous solution [42]. In this study, it was observed that the amount of fluoride adsorbed per mass of the adsorbent increased markedly with an increase in the free fluoride concentration when the soil-fluoride mixtures were kept for one week, but no explanation was given to it. The major shortcoming of soils is that they have low fluoride removal capacity but they have advantage over other defluoridating media in that they are locally available and cheap for application in developing countries like Ethiopia.

Most towns in the main Ethiopian Rift Valley have drinking water supplies with fluoride content much higher than the recommended value by WHO [20]. Fluoride removal from the available water is the only practical solution to minimize the problem of fluorosis. As already stated even though the adsorption capacity of soils is low, their availability in large amounts and low costs make them potential candidates for the defluoridation in remote areas. To our knowledge, no attempt has been made to compare the defluoridation ability of the soils with their chemical and mineralogical compositions. Therefore, one of the aims of this project is to investigate the correlation between these properties and defluoridation behaviors. It is also the aim of this project to investigate the adsorption of fluoride under various operating conditions and to study the kinetics of fluoride removal. The researches done so far have concentrated on the fluoride "removal capacity" of the soils based on total fluoride removed. No attempt has been made to do speciation analysis of the free fluoride and complexed fluoride. Thus, additionally it was tried to differentiate between free and complexed fluoride in the soil treated water samples. This is insofar of interest as aluminum fluoride complexes are supposed to cause Alzheimer's disease [43]. Therefore, the soils were also investigated with respect to aluminum-fluoride complexes in the water. The adsorption behavior of soils is better described by adsorption isotherm. Thus, it is also the aim of this project to draw

adsorption isotherm for long term defluoridation to describe the mechanism of fluoride removal by the soil under the investigation.

The electrochemical method could be used as an alternative defluoridation method in communities where electricity is available. Although there are some reports in the literature on the defluoridation of water by using aluminum electrode as an anode in an electrochemical cell [31, 32, 34], to our knowledge no systematic study of the electrochemical behaviors of aluminum electrode has been carried out and there were no documented data on the electrochemical behaviors of aluminum electrode. Thus, one additional aim of this project is to carryout some preliminary investigations on the electrochemical behaviors of aluminum that will enable us to identify the working potential range of the electrode. The results obtained will be used in conducting electrolysis of fluoride containing water.

2. THEORY

2.1 Aqueous chemistry of aluminum

Aluminum resists corrosion because of rapid formation of a coherent oxide or hydroxide film and not because of its position in the electrochemical series. The film is bonded firmly to the surface and is an excellent electrical insulator. Because of this aluminum, a very reactive metal which would otherwise oxidize very rapidly, is stable in air and is resistant to corrosion by sea water, many aqueous solutions and other chemical agents. MacDougall *et al.* [44] have shown that halide ions like chloride and bromide can give rise to local breakdown of the passive oxide film and subsequent pitting. The influence of different halide ions on the structure, composition, and general character of the passive oxide film has been the subject of much discussion. MacDougall *et al.* [44] hypothesized the following to explain how the above ions cause passivity breakdown:

i) incorporation of the ion into the oxide film lattice; ii) adsorption of the ions onto the oxide surface with subsequent chloride island formation and/or local thinning of the film; and
iii) interference with repair of the oxide film after local passivity breakdown, associated with chemical dissolution of the film and corresponding attack of the bare metal surface.

The existence range of $Al(OH)_3$ (s), which is important for removal of fluoride by anodic oxidation of aluminum, can be seen from the following Pourbaix diagram [45]. It is a potential versus pH diagram that shows a thermodynamically most stable species at a given pH and electrode potential.

Figure 2. Pourbaix diagram of aluminum at 25 ^{o}C, $C_{Al}^{3+} = 10^{-6}$ mol l^{-1}.

The figure shows the general corrosion characteristic of aluminum. As can be seen from the figure, aluminum corrodes over a substantial range of potential in acidic and alkali media but for $4 < pH < 9$, a very practical range for outdoor stability, it forms a highly protective passive layer. At a potential above the dashed line, water is not stable and is oxidized to oxygen gas and H^+ ,while below the lower dashed line hydrogen gas will be produced by the reduction of H^+ in water. Water is neither oxidized nor reduced in the potential range between these two dashed lines and hence can be used as a solvent in this potential range.

Aluminum tends to give up its three valence electrons to form a colorless aluminum cation, Al^{3+}. Because of its high positive charge, this is highly hydrated in water forming $[Al(H_2O)_6]^{3+}$. Aluminum in aqueous solutions rapidly and reversibly hydrolyses forming various monomeric hydrolysis products such as $[Al(OH)(H_2O)_5]^{2+}$, $[Al(OH)_2(H_2O)_4]^{+}$, $[Al(OH)_3(H_2O)_3]$ and $[Al(OH)_4(H_2O)_2]^{-}$ [46]. Fluoride ions can substitute in these complexes;

however, in neutral and alkaline solutions, aluminum has greater affinity for the hydroxide ions. The hydrolysis of aluminum forming monomeric species and the corresponding hydrolysis constant, K_h, are shown below:

$$[Al(H_2O)_6]^{3+} + H_2O \rightleftharpoons [Al(OH)(H_2O)_5]^{2+} + H_3O^+ \qquad K_h = 10^{-5.3} \qquad (1)$$

$$[Al(OH)(H_2O)_5]^{2+} + H_2O \rightleftharpoons [Al(OH)_2(H_2O)_4]^{+} + H_3O^+ \qquad K_h = 10^{-9.9} \qquad (2)$$

$$[Al(OH)_2(H_2O)_4]^{+} + H_2O \rightleftharpoons [Al(OH)_3(H_2O)_3] + H_3O^+ \qquad K_h = 10^{-15.6} \qquad (3)$$

$$[Al(OH)_3(H_2O)_3] + H_2O \rightleftharpoons [Al(OH)_4(H_2O)_2]^{-} + H_3O^+ \qquad K_h = 10^{-23.0} \qquad (4)$$

The form of monomeric aluminum species in solution depends on the pH. One can see the effect of pH on the distribution of aluminum species in water solution from Figure 3. The figure shows the pH range over which the various aluminum hydroxide complexes could exist.

Figure 3. Relationship between pH and mole fraction of different aluminum species, $C_{Al}^{3+} = 10^{-6}$ mol l^{-1}.

Both ^{19}F and ^{1}H NMR studies have shown that aqueous solution of AlF_3 contains six coordinate ions, $[AlF_x(H_2O)_{6-x})]^{3-x}$ where x = 0 - 6 depending on the fluoride concentration in the solution [47]. The overall stability constants,β, for the formation of the various aluminum fluoride complexes are given below:

$$Al^{3+}(aq) + F^{-}(aq) \rightleftharpoons AlF^{2+}(aq) \qquad \beta = 10^{6.3} \tag{5}$$

$$Al^{3+}(aq) + 2F^{-}(aq) \rightleftharpoons AlF_2^{+}(aq) \qquad \beta = 10^{11.5} \tag{6}$$

$$Al^{3+}(aq) + 3F^{-}(aq) \rightleftharpoons AlF_3(aq) \qquad \beta = 10^{15.5} \tag{7}$$

$$Al^{3+}(aq) + 4F^{-}(aq) \rightleftharpoons AlF_4^{-}(aq) \qquad \beta = 10^{17.7} \tag{8}$$

$$Al^{3+}(aq) + 5F^{-}(aq) \rightleftharpoons AlF_5^{2-}(aq) \qquad \beta = 10^{19.4} \tag{9}$$

$$Al^{3+}(aq) + 6F^{-}(aq) \rightleftharpoons AlF_6^{3-}(aq) \qquad \beta = 10^{19.7} \tag{10}$$

Figure 4 shows the variation of mole fraction of aluminum-fluoride complex as a function of pF. This helps us to identify which of the aluminum-fluoride complexes could be formed if the free fluoride concentration is known.

Figure 4. Plot of mole fraction of $AlF_x^{-(x-3)}$ as a function of pF where x = 0 - 6.

2.2 Lateritic soils

These soils are formed under tropical conditions of high rainfall and high temperature that is often seasonal. The term laterite is used as a common name for iron oxide rich tropical soils, which have been formed from weathering of rocks under strongly oxidizing and leaching conditions that leads to the removal of silica, alkalis and alkaline earth metals. This process, referred to as laterisation, leads to an accumulation of sparingly soluble compounds as the more soluble constituents of the parent rocks are leached out. The mineral compositions of lateritic soils vary greatly depending on the stage of laterisation. Lateritic soils, even when silica poor, may contain clay minerals, iron oxide minerals (goethite, hematite) and hydrated oxide of aluminum (gibbisite). In the final stage of laterisation, bauxite is formed. Laterites differ from clay soils in that aluminum is present as oxides or hydroxides instead of silicates [48-50].

3. EXPERIMENTAL

3.1 Sampling and sample preparation

The soil samples for defluoridation experiments were collected from Adiss Ababa, Gullale, Burayyu Brick Factory Compound and Ambo area (5 km west of Ambo town on the road to Nekemt). A soil sample from Hollota, which was already available in our laboratory, was used for comparison. Brick from Burayyu Brick Factory and clay pot bought from a market were tested in the same experiments. The soil samples are referred to as "red Gullale soil" (RGS), "yellow Gullale soil" (YGS), "Ambo soil" (AS), and "Hollota soil" (HS) in the following discussions. The soil samples were sun dried, crushed, ground and sieved to obtain particle sizes between 0.17-0.32 mm prior to the defluoridation experiments.

3.2 Thermal treatment

Twenty grams of RGS was transferred into a crucible and was then fired in a furnace (Carbolite, ELF model) at preset temperatures of 400, 500, 550, 600, and 800 ^{o}C for four hours. At the end of four hours, the thermally treated soil sample was taken out of the furnace, kept in a desiccator and allowed to cool to room temperature, and then weighed in order to determine the corresponding weight loss.

3.3 Preparation of solutions

A 0.1 mol l^{-1} NaF stock solution was prepared by dissolving 0.42 g of NaF (Riedel-de Haen, chem. pure) in distilled water. Other solutions, for the calibration of the fluoride selective electrode and for the electrolysis experiments, were prepared from this stock solution by dilution with distilled water. In order to determine the extent of complexed fluoride in the samples, calibration and determination were carried out by addition of Total Ionic Strength Adjustment Buffer (TISAB) prepared according to the procedure described in (Refs. [51, 52]). A 0.1 mol/l Na_2SO_4 solution was prepared by dissolving 14.2 g of the salt (NICE) in distilled water and was used as a supporting electrolyte in the electrochemical studies.

3.4 Experimental procedures

The fluoride ion selective electrode was calibrated prior to each experiment in order to determine the slope and intercept of the electrode which were in turn used to convert the experimentally obtained potential-time diagram to a concentration-time diagram by

$$C_F^- = 10^{(E\text{-const}) / S} \qquad (11)$$

where C_F^- is free fluoride concentration, E is the potential, S is the slope of the calibration curve and const is its intercept.

The defluoridation experiments were conducted at different contact time by adding 2 g of each adsorbent to 50 ml of aqueous fluoride solutions of different concentrations. The same

mass of the adsorbents and aqueous solution were used in all the experiments unless otherwise specified. The total fluoride ion concentration was determined potentiometrically by adding 10 ml of the TISAB to 10 ml of the standard or sample solution.

Electrolysis of 20 ml of 10^{-3} mol l^{-1} fluoride solutions were conducted in the cell constructed by ourselves at different applied potentials for 8000 s. Aluminum electrodes were used as both anode and cathode of the cell. The solutions were stirred during the experiments by using a magnetic stirrer. All the experiments were carried out at a laboratory temperature of 21 ± 3 ^{o}C.

3.5 Analytical methods

The soil samples were characterized by X-ray diffraction (XRD) spectrometry and X-ray fluorescence (XRF) spectrometry at University of Caliary, Italy and University of Karlsruhe**,** Germany. The fluoride ion concentration was measured potentiometrically with a fluoride ion-selective electrode (Orion Combination fluoride electrode, model 96-09) and conductivity/pH meter (Jenway Model 4330). The pH of the solutions was determined potentiometrically by a glass electrode.

The electrochemical studies of an aluminum electrode (d = 0.6 mm) were conducted with an Electrochemical Analyzer BAS 100W (Bioanlytical Systems Inc.). The investigations were carried out by utilizing 0.1 mol l^{-1} Na_2SO_4 as a supporting electrolyte without and with different NaF concentrations. Cyclic voltammetry, impedance spectroscopy and potentiometry were the methods of investigations.

4. RESULTS AND DISCUSSION

4.1 The electrochemical behavior of aluminum

4.1.1 General considerations

There are some reports found in the literature on defluoridation based on the electrochemically initiated dissolution of aluminum anodes [31, 32]. The mechanism of the fluoride removal seems to be based on the interaction of F^- with $Al(OH)_3$ and/ or removal of fluoride in the form of cryolite. The chemistry of the aqueous F^-/Al^{3+} system is rather complex and depends on the pH of the solution, on the total aluminum concentration in the system, and on the fluoride concentration. Thus the formation of the possible Al^{3+} hydroxo complexes together with the solubility equilibrium of $Al(OH)_3$ and the formation of the six possible fluoro complexes have to be considered (see Figure 3 and Figure 4). On the other hand, the corrosion of aluminum in aqueous solutions depends on the existence of a protecting layer of gibbsite ($Al_2O_3 \bullet 3H_2O$) the thermodynamic stability range of which is governed by the above mentioned equilibria. This is shown schematically in Figure 5.

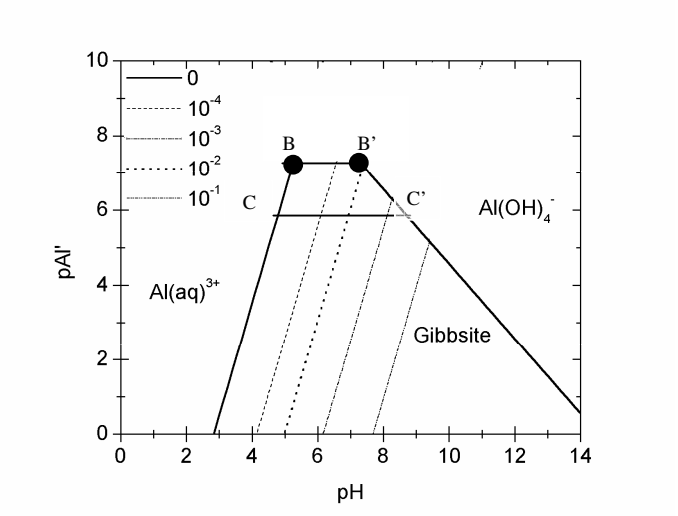

Figure 5. Simplified pAl' / pH diagram in the presence of fluoride at concentrations from 10^{-4} to 10^{-1} mol/l. The formation of monohydroxo and dihydroxo aluminates and soluble $Al(OH)_3$ have not been taken into consideration. In a first approximation it can be assumed that no solid phase exists above the line B B'.

It can be seen that the pH range within which gibbsite is stable is shortened with increasing fluoride concentration due to the formation of fluoro complexes. Taking the total aluminum concentration in the aqueous phase as 10^{-6} mol/l (line C - C' in Figure 5) the stability range decreases from $4.8 \leq pH \leq 9$ without fluoride to $7 \leq pH \leq 7.8$ in a solution containing 10^{-2} mol/l fluoride while in a 0.1 molar fluoride solution gibbsite is not formed and aluminum should dissolve by the reduction of water as it does at any pH outside the stability range of gibbsite. On the other hand, the conditions in the electrolysis cell have to be such that $Al(OH)_3$ precipitates in order to serve as adsorbent for fluoride. Unfortunately, these are the same conditions which will support the passivation of the aluminum electrodes leading to a high cell resistance and finally making the process uneconomical.

4.1.2 Voltammetric investigations of aluminum electrode

An aluminum disc electrode with a geometrical area of 2.8 x 10^{-3} cm^2 was utilized as working electrode. A Pt-wire was used as counter electrode and a silver/silver chloride electrode (1 molar in KCl) as reference electrode. A 0.1 molar solution of Na_2SO_4 served as supporting electrolyte. All measurements were carried out in air-saturated solutions. The aluminum electrode was polished on a nylon cloth prior to the measurements. Figure 6 shows a cyclic voltammogram obtained at an aluminum electrode in the supporting electrolyte.

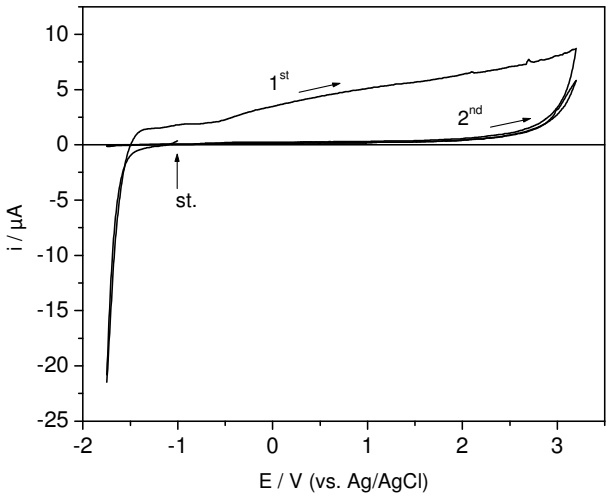

Figure 6. Cyclic voltammogram of an Al-electrode in 0.1 mol/l Na_2SO_4. Sweep rate: 0.1 V/s. The scan was started in the negative potential direction at –1 V (*st.*). Numbers in the votammogram refer to the respective cycles of the voltammogram.

The high cathodic current observed at potentials more negative than about -1.25 V is supposed to be due to the reduction of water that occurs at the very thin gibbsite layer formed on Al by both, air oxidation and interaction with water, after the polished electrode was inserted into the cell.

$$2H_2O + 2e^-(Al) \rightleftharpoons H_2 + 2OH^- \quad (12)$$

The potential range where hydrogen evolution is observed (E (vs. Ag/AgCl) < -1.2V) is in fair agreement with the value obtained from a rough thermodynamic estimation. The pH of the supporting electrolyte was found to be 5.8 thus the equilibrium potential of H_3O^+/H_2 will be -0.59 V. Taking the over potential of hydrogen at Al to be –0.6 V [53], we obtain about –1.2 V. This high cathodic current is not observed in the second cycle since the protecting gibbsite layer has grown while the electrode was polarized in the anodic region. In the 1st reverse cycle an increasing anodic current is obtained which we attribute to the growth of the gibbsite layer caused by the oxidation of aluminum at the gibbsite/Al interface due to the existence of pores. On scan reversal at +3.25 V, no considerable current flow is observed which holds for the successive cycles in both anodic and cathodic directions. This indicates that the protecting gibbsite layer has grown and thus its porosity has decreased. This situation changes in solutions containing fluoride as shown in Figure 7 and Figure 8.

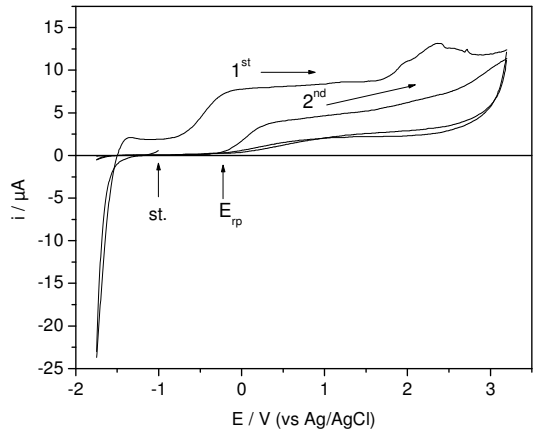

Figure 7. Cyclic voltammogram of an Al-electrode in 0.1 mol/l Na_2SO_4 + 0.001 mol/l NaF. All other conditions as in Figure 6. E_{rp} is repassivation potential. Numbers in the voltammogram refer to the respective cycles.

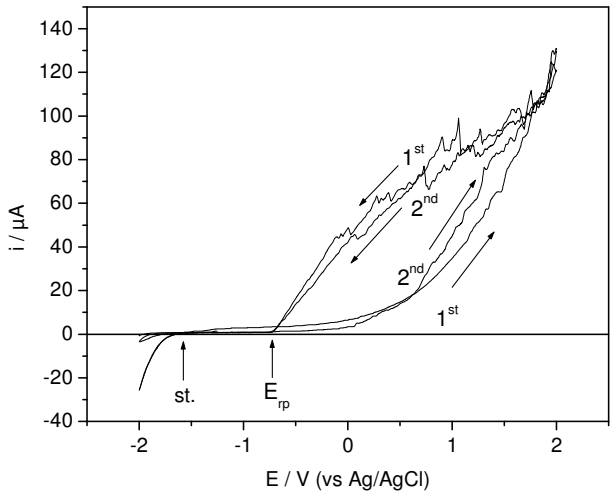

Figure 8. Cyclic voltammogram of an Al-electrode in 0.1 mol /l NaF. All other conditions as in Figure 6. Numbers in the voltammogram refer to the respective cycles.

There is no significant difference seen between the voltammograms shown in Figure 6 and Figure 7 due to the presence of 0.001 mol/l fluoride in the potential range E < -0.2 V while the anodic current in the 1st potential scan is increased at potentials more positive than about -0.5 V. This anodic current is observed in successive cycles as well and is an indication for a breakdown of the protective gibbsite layer. Passivation is restored at potentials more negative to the repassivation potential at -0.235 V. The voltammogram obtained in a 0.1 mol/l NaF solution (Figure 8) shows the typical pattern, which is expected if a metal goes from the passivated state into the transpassive anodic potential region. The repassivation occurs at a more negative potential (-0.720 V) due to the increase in fluoride concentration. Further voltammograms were recorded in stirred and quiet solutions in order to investigate the dependence of the breakdown current on the transport of fluoride ion to the electrode. Figure 9 clearly shows the influence of the transport of fluoride to the electrode.

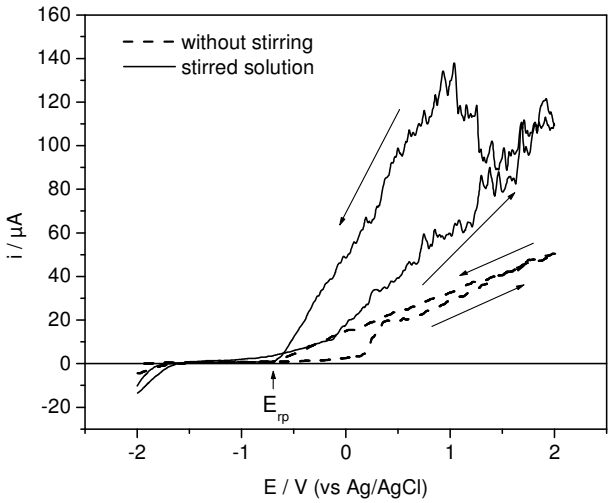

Figure 9. Cyclic voltammogram of an Al-electrode in 0.1 mol /l NaF in unstirred and stirred solution. All other conditions as in Figure 6.

The anodic current at 2.00 V has doubled due to the stirring of the solution, which indicates that the breakdown is controlled by the fluoride ion transport to the electrode and less likely by the reaction rate or diffusion through pores in the protecting layer toward the aluminum. On the other hand, no change in E_{rp} (-0.75 V) is observed due to stirring.

4.1.3 Impedance spectroscopic investigation of aluminum electrode

It is hardly possible to suggest a reaction scheme responsible for the anodic current in the transpassive potential region based on experimental results obtained by cyclic voltammetry only. If the system aluminum/gibbsite/solution is represented by an electrical equivalent as shown below:

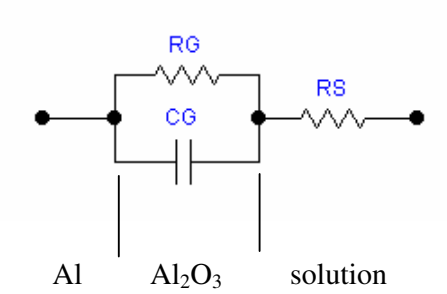

where RG is the resistance of the gibbsite layer, CG the corresponding capacitance and RS the solution resistance, impedance spectroscopy can be utilized in order to investigate the influence of fluoride on the growth of the gibbsite layer. These experiments were carried out within the passive potential region at -1.250 V. The electrode was kept at this potential throughout each experiment and measurements were taken in time intervals of 10 minutes**.** Figure 10 shows the impedance dispersion (Cole/Cole plot) obtained in Na_2SO_4 and in Na_2SO_4 + 0.001 mol/l NaF as examples.

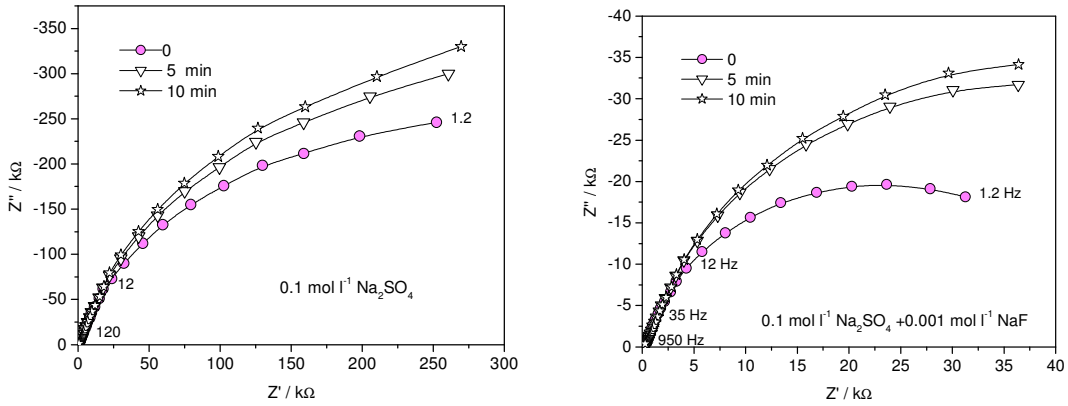

Figure 10. Impedance dispersion of aluminum in 0.1 mol/l Na_2SO_4 and in 0.1 mol/l Na_2SO_4 + 0.001 mol/l NaF at –1.250 V.

Frequency range: 1.2 Hz to 950 Hz.

ac Amplitude: 5 mV.

The numbers in the graph are ac frequencies in Hz. .

The experimental data were evaluated utilizing the software "Equivalent Circuit 3.51" [54]. The results are compiled in Table 1.

Table 1. Resistance and parallel capacitance of the gibbsite layer at –1.250 V calculated from the impedance dispersion data.

Solution	t / min	R / MΩ	C / μF cm^{-2}
0.1 mol/l Na_2SO_4	0	0.96	29
	10	1.18	30
	20	1.3	36
0.1 mol/l Na_2SO_4 + 0.001 mol/l NaF	0	0.58	46
	10	0.74	54
	20	0.85	57
0.1 mol/l NaF	0	0.35	45
	10	0.33	44
	20	0.09	27

Since the resistance is directly proportional to the thickness of the protecting layer and assuming that the area and resistivity, ρ, are independent of the composition of the electrolyte solution, it can be concluded from the values in Table 1 that in the presence of 0.1 mol/l fluoride ion the growth rate is slower than the dissolution rate. Assuming that the gibbsite layer is impermeable for water and ions but permeable for oxygen the layer will grow inward.

The layer will increase proportional to the rate of O_2 diffusion through it. Thus the rate of gibbsite formation is given by

$$\frac{dn}{dt} = D\,A\frac{C_O(w)}{x} \tag{13}$$

where D is the diffusion coefficient of O_2 in the oxide, A is the area of the electrode, $C_O(w)$ is the concentration of O_2 in the electrolyte and x is the thickness of the oxide layer. In eqn. (13) it has been assumed that the chemical reaction of O_2 with Al is fast and therefore the concentration of oxygen at the aluminum/gibbsite interface is zero. The increase in thickness, dx, is given by

$$dx = k'\,dn \tag{14}$$

where k' is a proportionality constant and dn is the amount of O_2 reaching the interface between gibbsite and aluminum. Combining eqn. (13) and eqn. (14) and introducing $k = k'\,D\,A\,C_O(w)$

$$\frac{dx}{dt} = \frac{k}{x} \tag{15}$$

is obtained. Integration of eqn. (15) together with the initial conditions $(t = 0\,,\ x = 0)$ yields

$$x = \sqrt{2\,k\,t} \tag{16}$$

If the experimentally obtained resistance of the aluminum electrode is plotted vs. square root time (Figure 11) the linear relationship seems to hold for fluoride free solutions and low fluoride concentrations. The situation changes in solutions with a relatively high fluoride ion concentration. It can be assumed that the dissolution of gibbsite at the gibbsite/electrolyte interface is faster than the growth rate at the $Al/Al_20_3 \bullet 3H_2O$ interface. The decreasing thickness in turn will increase the rate of O_2 diffusion. A steady state might be reached at moderate fluoride concentrations.

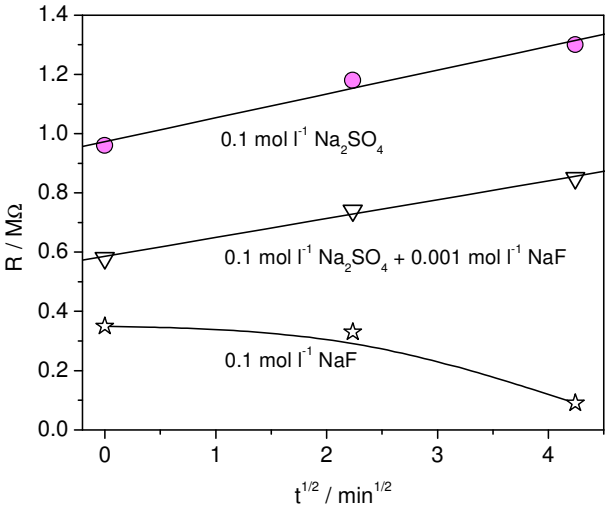

Figure 11. Dependence of the gibbsite layer resistance on the square root of time.

The primary step in the reaction of fluoride with gibbsite should be the adsorption of fluoride ion on the gibbsite layer followed by complexation of aluminum ion. The result of the adsorption will be a surface excess of negative charges, which in turn should be reflected by a negative current less potential of the aluminum electrode. The experimental results shown in Figure 12 verify this assumption.

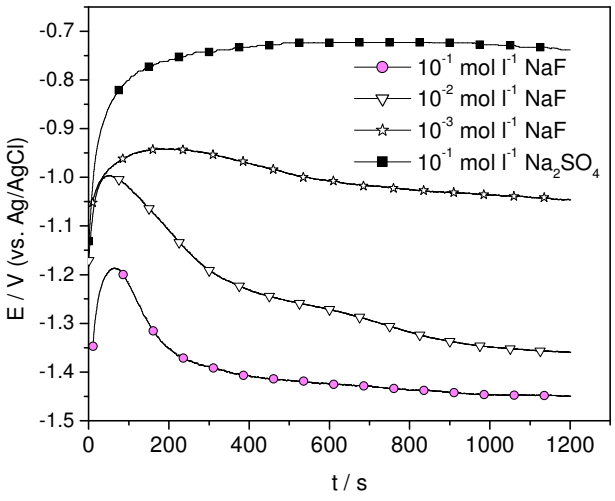

Figure 12. Potential – time behavior of aluminum electrodes in stirred solutions containing different fluoride ion concentrations.

4.1.4 Potentiometric investigations of aluminum electrode

These preliminary experiments were carried out in order to investigate whether potentiometric investigations at oxide covered electrodes can be used to shed some light to the understanding of the processes involved in the adsorption of fluoride ion on clays and lateritic soils. Obviously this method seems to be promising but needs further investigation, which was not the aim of this project.

Nevertheless, from the experimental findings a reaction scheme for the voltammetric behavior of aluminum electrodes can be proposed. The reactions to be taken into account are those occurring at the gibbsite/solution interface and at the aluminum/gibbsite interface and are independent as long as the protecting oxide layer is flawless.

The solubility of gibbsite can be increased due to the involvement of the Al^{3+} in side-reactions. There are two side-reactions to be accounted for in the system under consideration. Aluminum ion can form hydroxo complexes and in a fluoride containing solution fluoro complexes as well. The conditional solubility product, $K_s^{'} = K_s(\alpha_F + \alpha_{OH})$, characterizes the effect of the side-reaction on the solubility of gibbsite, where α_F and α_{OH} are the side-reaction coefficients [55] accounting for the formation of the fluoro and hydroxo complexes respectively. The overall reaction for the dissolution of gibbsite in a fluoride containing solution can be formulated as:

$$Al_2O_3 \bullet 3H_2O + 2nF^- \rightleftharpoons 2AlF_n^{(3-n)} + 6OH^- \qquad (17)$$

The dissolution will cause a local increase in pH due to the hydroxide ions liberated but since the diffusion of hydroxide from the interface into the bulk of the electrolyte is much faster than the diffusion of fluoride to the interface the pH change will be somewhat level off. On the other hand, there will be a shift of the equilibrium to the gibbsite side due to the pH increase. With the justified assumption that the dissolution process is diffusion controlled as long as the aluminum is kept at rather negative potentials, the rate of dissolution is determined by the concentration gradient between the bulk and the gibbsite surface. When the electrode potential becomes more positive, negative charges are required at the gibbsite/solution interface to compensate for the positive charges injected at the aluminum/gibbsite interface. This leads to an excess of fluoride ion and hence to a shift in the dissolution equilibrium. The growth of the oxide layer can no longer compensate the loss due to the dissolution. The increasing current and the current fluctuations observed in the voltammogram indicate this

breakdown of the passivation. A possible reaction scheme after the breakdown can be formulated as follows:

the active dissolution of aluminum

$$2Al + 6H_2O \rightleftharpoons 2Al^{3+} + 3H_2 + 6OH^- \quad \text{(chemical)} \tag{18}$$

the electrochemical oxidation of H_2

$$H_2 + 2H_2O \rightleftharpoons 2H_3O^+ + 2e^-(Al) \quad \text{(electrochemical)} \tag{19}$$

the hydrolysis and complexation of Al^{3+}

$$Al^{3+} + 2nH_2O \rightleftharpoons Al(OH)_n^{(3-n)} + nH_3O^+ \quad \text{(chemical)} \tag{20}$$

$$Al^{3+} + nF^- \rightleftharpoons AlF_n^{(3-n)} \quad \text{(chemical)} \tag{21}$$

The precipitation of $Al(OH)_3$ is also possible if the pH and fluoride concentration are such that aluminum hydroxide is thermodynamically stable. The fluoride removal is finally based on the adsorption of fluoride ion on the $Al(OH)_3$. Since the application of the electrolysis is aimed at the defluoridation of water, a few potentiostatic electrolysis experiments were carried out. The initial fluoride concentration was 1 mmol/l. 20 ml solution was taken for the experiments. Aluminum electrodes served as anode and cathode. The solution was stirred during the electrolysis. The charge consumed in the electrolysis was obtained by integration of the current/time curves recorded. The results are summarized in Table 2.

Table 2. Results obtained by electrolyzing 20 ml of 1 mmol/l NaF solution for 8000 s at a cell voltage of 2.0 V, 2.5 V and 3.0 V.

Cell voltage/ V	Charge consumed/ C	Initial pH	Final pH	Final F^-/ mmol l^{-1}	% removed
2	5.36	7.7	8.9	0.58	42
2.5	9.73	7.7	9.21	0.53	47
3	10.73	7.7	9.26	0.32	68

Precipitation of $Al(OH)_3$ was observed around the anode and gas evolution at both electrodes. Since there are definitely side-reactions involved in the formation of $Al(OH)_3$, a comparison of charge consumed and amount of fluoride removed seems to be unreasonable. The appreciable increase in pH is an interesting observation but difficult to explain. In order to make a judgment about the potential of electrolysis for the defluoridation further investigations are required.

4.2 Fluoride removal by adsorption on lateritic soils

4.2.1 Characterization of the soil samples

The soil samples were analyzed by X-ray diffraction (XRD) and X-ray fluorescence (XRF) spectrometry. The following minerals were identified from the peak characteristics of X-ray diffraction analysis:

RGS: quartz, plagioclase, disordered kaolinite, iron oxide, dickite.

YGS: quartz, potassium feldspar**.**

AS: quartz, traces of plagioclase and goethite.

HS: quartz, halloysite, kaolinite (disordered), amorphous iron oxide.

The chemical composition of the soil samples based on the results of XRD and XRF analysis are shown in Table 3.

Table 3. Chemical composition of the soil samples.

Soil	Quartz %	Feldspar %	Calcite %	Dolomite %	Illite %	Kaolinite %	Montmorillonite %	Al_2O_3 %	Fe_2O_3 %
AS	22	7	3	5	12	9	30	3.1	7.8
YGS	19	52	0	7	5	?	5	5	6.23
RGS	17	9	0	0	5	?	31	22.68	13.09

The results of XRD spectroscopic analysis of the soil samples show that all the samples contained quartz which has hardly any defluoridating capacity. Essayas, A. [27] has shown that coarse constituents of his clay samples like quartz, mica, muscovite and microcline had no defluoridation capacity. If the amounts of Fe_2O_3 and Al_2O_3 are taken as an indication of the extent of laterisation of the soils, the RGS is the most lateritic soil and the extent of laterisation in AS and YGS is nearly the same.

4.2.2 Comparison of defluoridation capacity of untreated soil samples

In this study it was intended to choose the soil with the highest fluoride removal capacity for further investigations. HS was taken only for comparison. In order to classify the soils with respect to their defluoridation capacity, the amount of fluoride removed within 4000 s was measured. Two grams of the respective soil was suspended in 50 ml of 0.99 mmol l^{-1} fluoride solution and the decrease in free fluoride concentration was monitored potentiometrically (Figure 13).

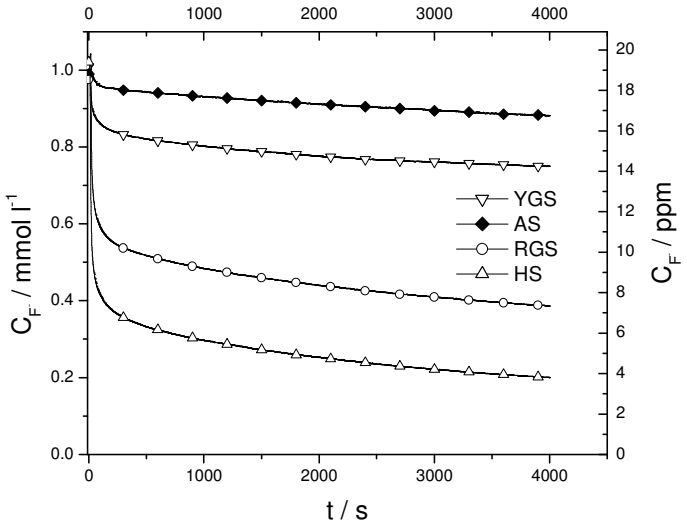

Figure 13. Change in free fluoride ion concentration with time observed for different soils.

Based on the free fluoride concentration remaining in the solution we may group the soils in AS and YGS on one side and RGS and HS on the other. The determination of the total fluoride at the end of the experiment reflects a different picture. The results of the experiment are compiled in Table 4.

Table 4. Effect of different adsorbing media on the removal capacity for the defluoridation of 0.99 mmol l^{-1} fluoride solutions.

Soil	Initial F^-/ mmol l^{-1}	Free F^-/ mmol l^{-1}	Complexed F^-/ mmol l^{-1}	Total F^-/ mmol l^{-1}	F^- adsorbed/ mmol/ kg	Final pH
AS	0.99	0.88	0.01	0.89	2.5	8.85
YGS	0.99	0.75	0.15	0.90	2.3	5.69
RGS	0.99	0.38	0.29	0.67	8.1	6.07
HS	0.99	0.19	0.22	0.41	15	5.66

The order YGS ≅ AS < RGS < HS is obtained with respect to the amount of fluoride adsorbed per gram of the soil. On the other hand, there is a significant difference in the amount of complexed fluoride in water between the soils and it is noticeable that there seems to be a correlation between fluoride adsorption and complexation of fluoride in water. The order observed for YGS, AS and RGS is well in line with the results of the chemical analysis and the mineral composition of the soils if it is assumed that the active components for fluoride adsorption are aluminum oxide and iron (III) oxide. Taking only these components into account, the active components in 2 g soil are about 0.2 g in YGS and AS but 0.7 g in RGS values which correlate fairly well with the adsorbed amount of fluoride. The amount of

complexed fluoride expected in water can be calculated on the basis of the free fluoride concentration and the pH of the solution. The source of aluminum ion is supposed to be gibbsite present in the clay. In the presence of fluoride the solubility of gibbsite is increased as discussed in section 4.1.1 of the thesis. The side-reaction coefficient, $\alpha_{F,}$ that takes the complexation of Al^{3+} into account can be calculated on the basis of the free fluoride concentration and the formation constants of the complexes. Taking RGS as an example we obtain $\alpha_F = 2.31 \times 10^5$. With $\log K_{sp} = -33.5$ the total aluminum ion concentration is calculated to be 0.073 mmol l^{-1} at pH 6. It follows from Figure 3 that at a free fluoride concentration of 0.38 mmol l^{-1} the difluoro, trifluoro and tetrafluoro complexes of aluminum exist in a ratio 0.3, 0.65 and 0.05 respectively. Thus, the complexed fluoride ion concentration is obtained to be 0.20 mmol l^{-1} a value which is in good agreement with the experimentally determined concentration. The high complexed fluoride concentration for RGS may be attributed to the presence of relatively high amount of Al_2O_3 which may dissolve in fluoride containing solution thereby releasing aluminum ion capable of complexing fluoride ions. Recent study on mice [22] has shown that aluminum fluoride complexes mimic the action of many neurotransmitters, hormones and growth factors and thus can affect cellular responses. They were also found to affect the activities of a variety of enzymes, produced change in the brain involving change in the concentration of the free radical scavenger's glutathione as well as reduced ascorbic acid concentration, 0.29 mmol l^{-1}. This implies that the complexed fluoride has also a significant impact on health and should be given due attention during analysis.

As can be seen from Table 4, the removal efficiencies of AS and YGS are too low for application to practical purposes. Due to this reason, further experiments were not conducted using these soil samples and only RGS was used in the subsequent studies.

4.2.3 Effects of thermal treatment

The aim of these experiments was to see the influence of thermal treatment on the removal efficiency and removal capacity of RGS. Two grams of each adsorbent was suspended in 50 ml of 0.99 mmol l^{-1} fluoride solution. The experiments were conducted over 4000 s. Figure 14 shows the effect of thermal treatment on the defluoridation behaviors of RGS. The results of these experiments are summarized in Table 5.

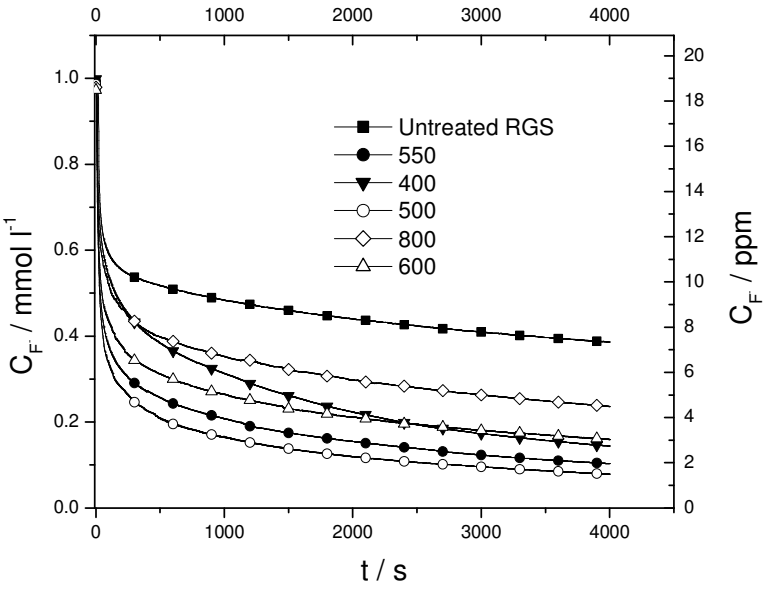

Figure 14. Change in free fluoride ion concentration with time for defluoridation by untreated RGS and RGS fired at different temperatures. The numbers in the Figure indicate the firing temperatures in ^{o}C.

Table 5. Effect of thermal treatment on removal efficiency and adsorption capacity for the defluoridation of 0.99 mmol l^{-1} fluoride solutions.

Temperature/ ^{o}C	Free F^-/ mmol l^{-1}	Complexed F^-/mmol l^{-1}	Total F^-/ mmol l^{-1}	F^- adsorbed/ mmol/kg	% removed
Untreated	0.38	0.29	0.67	8.1	32
400	0.14	0.049	0.19	20	81
500	0.078	0.26	0.34	16	66
550	0.10	0.37	0.47	13	53
600	0.16	0.34	0.50	12	49
800	0.24	0.32	0.56	0.011	43

As can be seen from Table 5, the highest removal efficiency and removal capacity was observed for the sample treated at 400 ^{o}C but further increase in temperature reduces the removal efficiency and removal capacity. The high removal efficiency and removal capacity at 400 ^{o}C may be attributed to the formation of activated alumina from gibbisite. The 2.56% weight loss at 400 ^{o}C (Figure 15) may be attributed to the removal of surface water from the soil. Constitutional water is lost in the temperature range 400-550 ^{o}C (about 11%) which is accompanied by a sharp increase in weight loss. The decline in the fluoride removal efficiency at higher treatment temperatures is probably caused by the change in the soil-mineral structures. At temperature above 700 ^{o}C, clay minerals such as kaolinite, montmorillonite and illite loose all the constitutional OH and finally their layered structures are disrupted and can't be reconstituted by rehydration [56]. The percent removal and percent weight loss for RGS as a function of the firing temperatures are given in Figure 15 below.

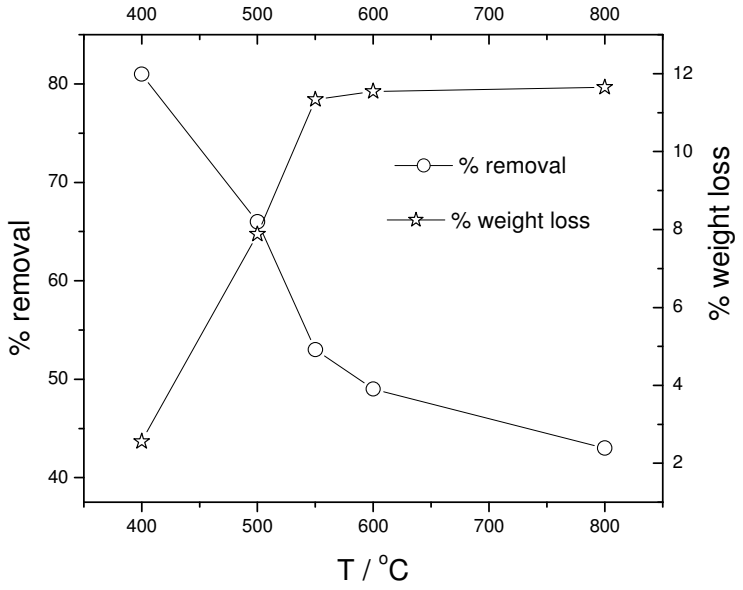

Figure 15. Percent removal and percent weight loss for RGS as a function of firing temperature.

The figure clearly shows that the highest removal efficiency was observed at 400 ^{o}C and thereafter starts to decline with increase in firing temperature. It can also be seen that the percent weight loss after 550 ^{o}C is more or less constant. This may be due to the complete removal of all constitutional water molecules.

Clays, fired at relatively lower temperatures, have long been used for making pot, bricks and other clay wares in different parts of Ethiopia. Since RGS could be used for the same purpose, comparative defluoridation study was carried out by using ground clay pot and ground brick as adsorbents.

Figure 16 shows the variation of free fluoride concentration for defluoridation of 0.99 mmol/l fluoride solution by using 2 g of untreated RGS, RGS fired at 500 ^{o}C, ground brick and ground clay pot for a contact time of 4000 s.

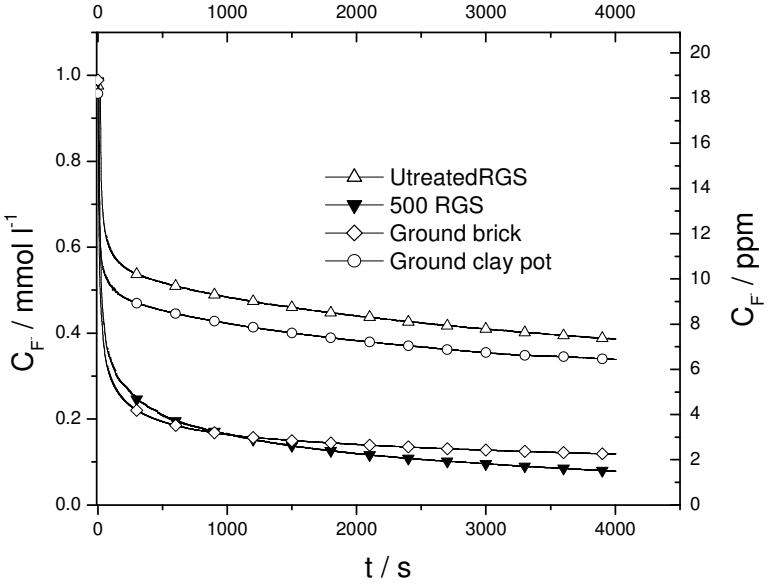

Figure 16. Change in free fluoride ion concentration with time for defluoridation of 0.99 mmol l^{-1} fluoride solutions by untreated RGS, RGS fired at 500 ^{o}C, ground clay pot, and ground brick.

The figure shows that RGS fired at 500 ^{0}C have the highest fluoride removal capacity followed by ground brick and clay pot respectively. As can be seen from the figure, although the fluoride removal capacity of ground brick is less than that of RGS fired at 500 ^{o}C it has the highest fluoride removal rate. The removal efficiency and the amount of fluoride adsorbed per unit mass of each of the above adsorbents are given in Table 6.

Table 6. The removal efficiency and amount of fluoride adsorbed per kg of the adsorbent for defluoridation of 0.99 mmol l^{-1} fluoride solutions by untreated RGS, RGS fired at 500 ^{o}C, ground brick and ground clay pot.

Adsorbent	Initial F^-/ mmol l^{-1}	Free F^- / mmol l^{-1}	Complexed F^-/ mmol l^{-1}	Total F^-/ mmol l^{-1}	F^- adsorbed/ mmol/kg	% removed
Untreated RGS	0.99	0.38	0.29	0.67	8.1	32
RGS fired at 500 ^{o}C		0.078	0.26	0.34	16	66
Ground brick		0.12	0.28	0.40	15	60
Ground clay pot		0.34	0.29	0.63	9.1	36

The table shows that the removal efficiency of the adsorbents increases in the order untreated RGS, ground clay pot, ground brick and RGS fired at 500 ^{o}C. It also shows that the fluoride removal efficiencies of ground clay pot and ground brick are greater than that of untreated RGS. This may indicate that thermal treatment is important for better defluoridation. It can also be seen that the amount of fluoride complexed is comparable for all the adsorbents.

4.2.4 Effect of initial fluoride concentration

The effects of the initial fluoride concentrations on the adsorption of fluoride were studied by varying the initial fluoride concentrations in the range 0.99-3.85 mmol l^{-1} at a constant contact time and adsorbent dose. The adsorbents used in this study were untreated RGS, RGS fired at 500 ^{o}C, ground clay pot and ground brick. 2 g of each adsorbent was used. The results obtained by using different adsorbents and different initial fluoride concentrations are given in Figures 17A-17D and compiled in Table 7.

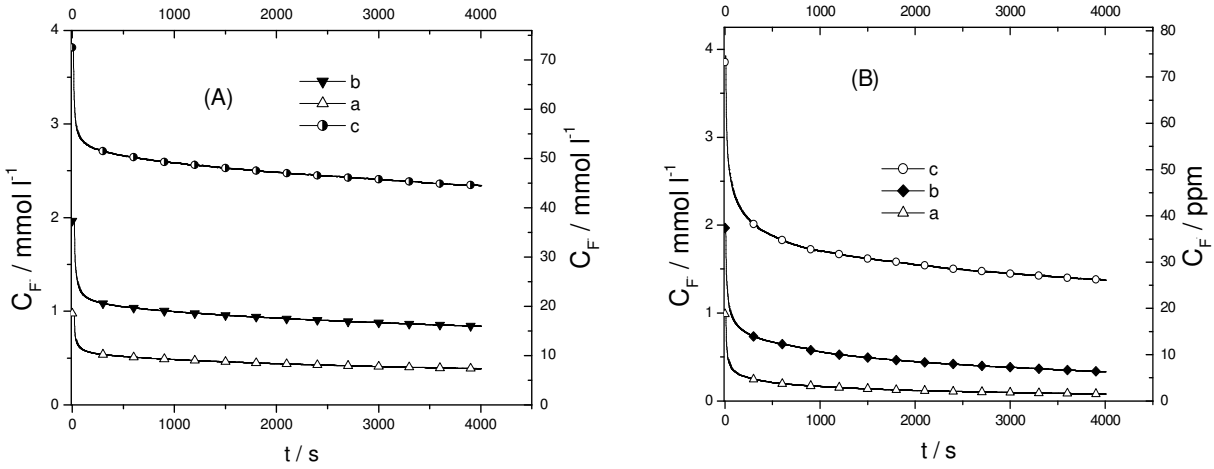

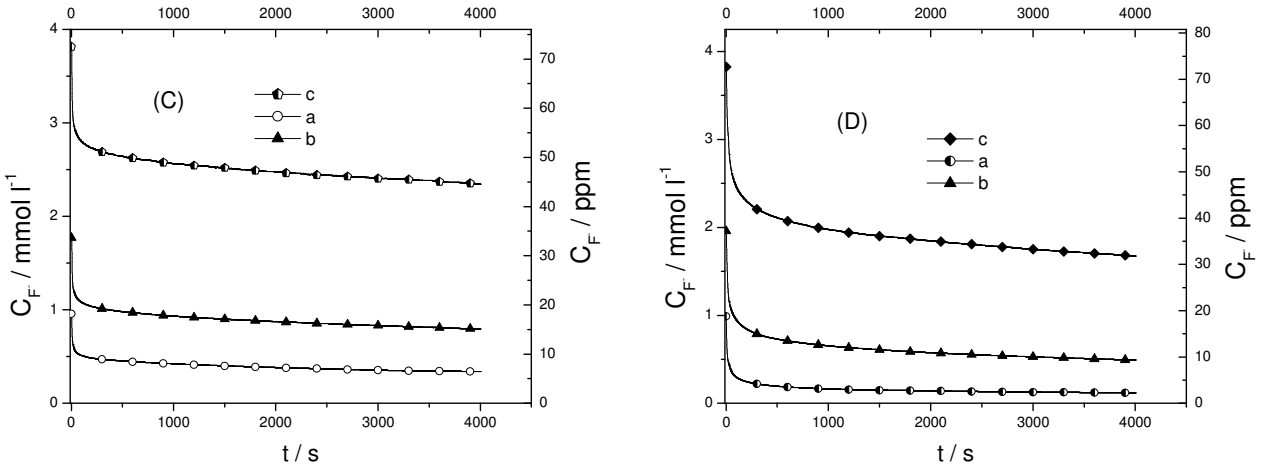

Figure 17. Change in free fluoride ion concentration with time for defluoridation by A) untreated RGS; B) RGS fired at 500 ^{o}C; C) ground clay pot; D) ground brick; at different initial fluoride concentrations. (Note a = 0.99; b = 1.96; and c = 3.85 mmol l^{-1} initial fluoride concentration)

It was observed that the fluoride removal efficiency increases with decreasing initial fluoride concentration for constant adsorbent dose and contact time as can be seen from Figures 17A-17D and Table 7. This is in accordance with the findings of Hayatolla, I. H. [26]. The decrease in removal efficiency at higher initial fluoride concentrations is due to the saturation of the active sites of the adsorbent.

Table 7. Effect of initial fluoride concentration on the adsorption capacity and removal efficiency of different adsorbents.

Adsorbent	Initial F^-/ mol l^{-1}	Free F^-/ mmol l^{-1}	Complexed F^-/mmol l^{-1}	Total F^- /mmol l^-	F^- adsorbed/ mmol/kg	% removed
Untreated RGS	0.99	0.38	0.29	0.67	8.1	32
	1.96	0.84	0.55	1.4	15	29
	3.85	2.3	0.48	2.8	27	27
RGS fired at 500 ^oC	0.99	0.078	0.26	0.34	16	66
	1.96	0.33	0.39	0.72	32	63
	3.85	1.4	0.48	1.9	51	51
Ground clay pot	0.99	0.34	0.26	0.60	10	40
	1.96	0.79	0.50	1.3	17	34
	3.85	2.4	0.42	2.8	27	27
Ground brick	0.99	0.12	0.28	0.40	15	61
	1.96	0.49	0.45	0.94	26	52
	3.85	1.7	0.50	2.2	43	43

As can be seen from Table 7, fluoride removal efficiency increases with decreasing initial fluoride concentration for a constant adsorbent dose and contact time. However, the total capacity of the adsorbents increases when the initial fluoride concentrations in the concentration range studied are increased. This can be attributed to the utilization of the less accessible or energetically less active sites because of increase in diffusivity and activity of

fluoride ion upon increasing initial fluoride concentration. The interior of the porous adsorbents contain more sites than exteriors. However, the sites present on the interior surface of a pore may not be as easily available as the sites on the exterior surface because of the resistance to the pore diffusion [57].

4.2.5 Effect of adsorbent mass

The effect of adsorbent mass on the fluoride removal efficiency was studied by varying mass of the adsorbents viz 2, 4, 6 and 8 g. The adsorbents investigated in this experiment were RGS fired at 500 ^{o}C, ground clay pot and ground brick. The results obtained for different adsorbents and their respective different masses are shown in Figures 18a-18c, Figure 19 and Table 8. The numbers in the Figures indicate the masses of the adsorbent in gram.

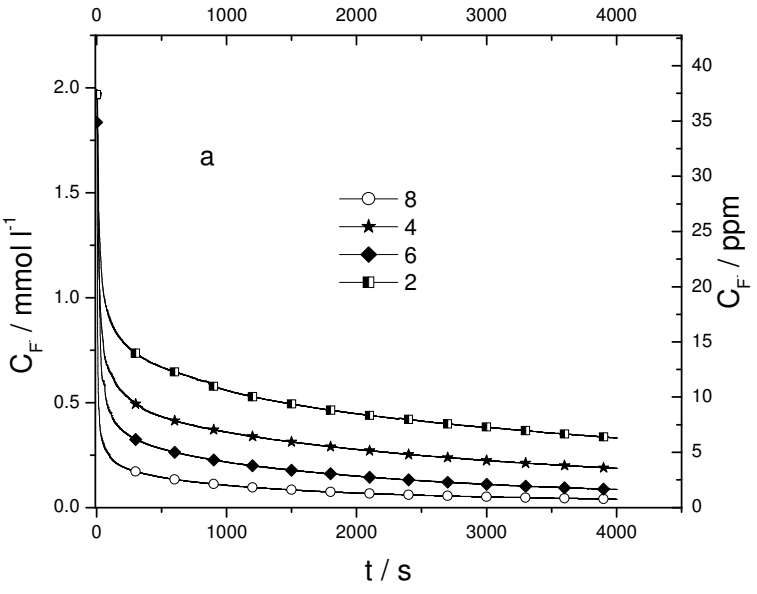

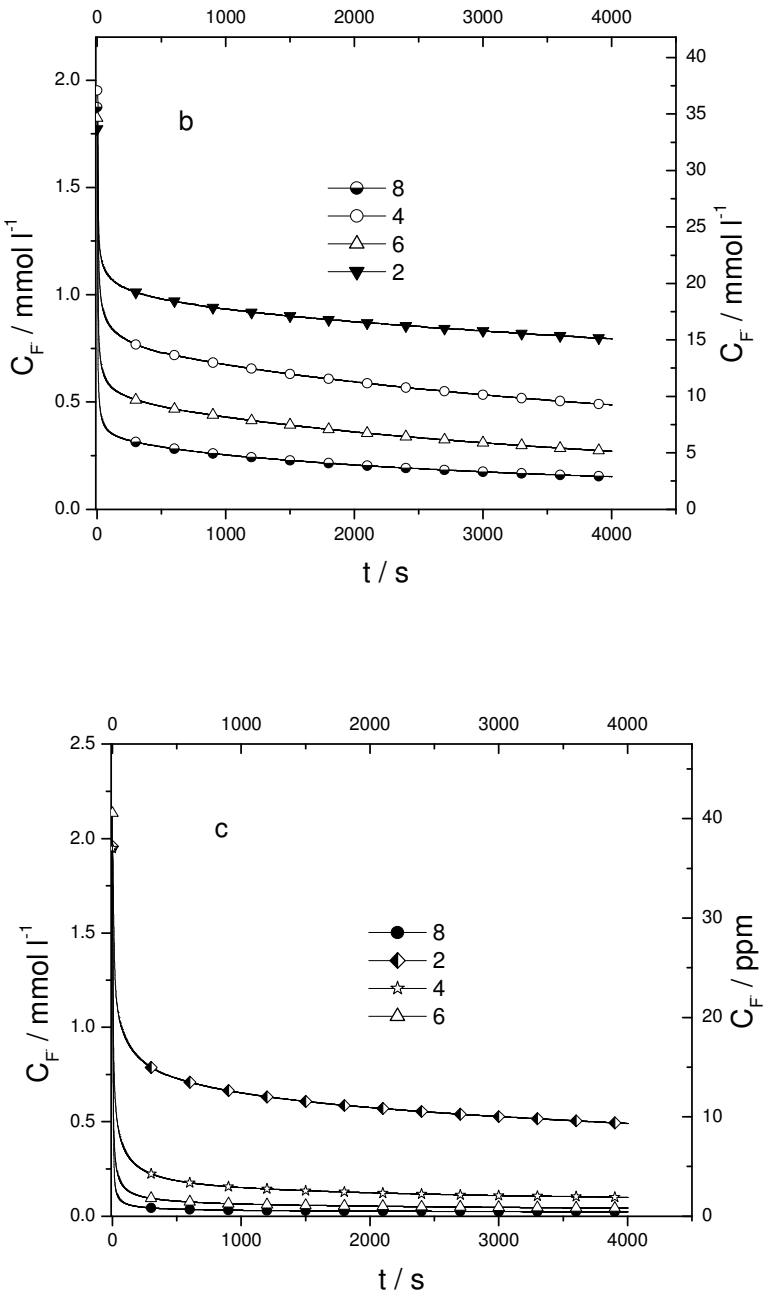

Figure 18. Change in free fluoride ion concentration as a function of time for defloridation of 1.96 mmol l^{-1} F^- solutions by different masses of a) RGS fired at 500 ^oC; b) ground clay pot; and c) ground brick.

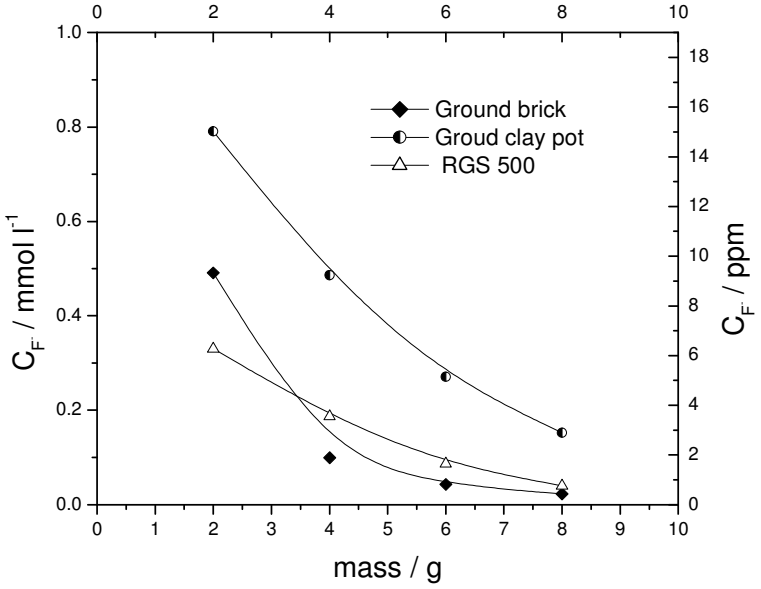

Figure 19. Residual fluoride concentration as a function of mass of different adsorbents for defluoridation of 0.99 mmol l^{-1} fluoride solutions by RGS fired at 500 ^{o}C, ground clay pot and ground brick.

Table 8. Effect of adsorbent dose on removal efficiency and adsorption capacity for the defluoridation of 1.96 mmol l^{-1} fluoride solutions by using RGS fired at 500 ^{o}C, ground clay pot and ground brick.

Adsorbent	Mass of the adsorbent/g	Initial F^-/ mmol l^{-1}	Free F^- / mmol l^{-1}	Complexed F^-/mmol l^{-1}	Total F^-/ mmol l^{-1}	F^- adsorbed/ mmol/kg	% removed
RGS fired at 500 ^{o}C	2	1.96	0.33	0.39	0.72	32	63
	4		0.19	0.22	0.41	39	79
	6		0.086	0.13	0.22	44	89
	8		0.04	0.075	0.12	47	94
Ground clay pot	2		0.79	0.29	1.1	22	44
	4		0.48	0.47	0.95	26	51
	6		0.27	0.41	0.68	33	65
	8		0.15	0.31	0.46	38	77
Ground brick	2		0.49	0.45	0.94	26	52
	4		0.099	0.35	0.45	39	77
	6		0.043	0.31	0.35	41	82
	8		0.023	0.24	0.26	44	87

The quantity of the adsorbent significantly influenced the extent of defluoridation as reflected by the measured residual fluoride concentration at equilibrium as can be seen from Figures 18a-18c, Figure 19 and Table 8. All the figures and the table show that the fluoride removal efficiency and adsorption capacity increase significantly with the adsorbent dose for a constant initial fluoride concentration and constant contact time. This is due to an increase in active

sites of the adsorbent with a corresponding increase in its mass (dose). The total fluoride ion concentration in the defluoridation of the above fluoride solution has decreased from 0.72 mmol l^{-1} (13.7 ppm) to 0.12 mmol l^{-1} (2.3 ppm) when the mass of RGS fired at 500 ^{o}C adsorbent was increased from 2 g to 8 g. This shows that it is possible to reduce the fluoride concentration in drinking water to a recommended or even lower value by using appropriate mass of the adsorbent. Table 8 also shows that the concentration of complexed fluoride decreases with an increase in the mass of the adsorbents.

4.2.6 Effect of contact time

The effect of contact time on fluoride removal was investigated by varying the contact time while holding the initial fluoride concentration and adsorbent dose constant. The experiments were conducted by using 2 g of RGS fired at 500 ^{o}C as an adsorbent. The results of defluoridation carried out for contact time of 4000, 8000, 12,000 s are summarized in Table 9.

Table 9. Effect of contact time on the fluoride removal efficiency for defluoridation of 1.96 mmol l^{-1} fluoride solutions by using RGS fired at 500 ^{o}C as an adsorbent.

Initial F^- / mmol l^{-1}	Contact time/ s	Total F^- / mmol l^{-1}	% removed
1.96	4000	0.72	63
	8000	0.63	68
	12000	0.57	71

Results of Table 9 show that fluoride removal efficiency increases with an increase in contact time. However, the increase was not as such significant for longer contact times. This indicates that longer contact time has no much significance since the reaction is fast during the initial minutes. Allowing more time does not bring much gain in fluoride uptake (removal) by the media, if any then not significant. It was also noted that the efficiency is high at low fluoride concentration and decreases with increasing fluoride concentration irrespective of the contact time. Results of all the tables presented so far indicated that a certain amount of fluoride ion remains in water by forming complex with metal cations.

Defluoridation experiments were also carried out over a long time by shaking the fluoride-RGS soil mixture for 72 h over a flask shaker (Gallenkamp). In these experiments 2 g of the RGS were added to 50 ml fluoride solutions whose initial concentrations are indicated in Table 10. The results obtained are compiled in Table 10 and the corresponding adsorption isotherm is depicted in Figure 20.

Table 10. Results of defluoridation experiment conducted for 72 h.

Contact time/h	Initial F^- / mol l^{-1}	Free F^-/ mmol l^{-1}	Complexed F^-/ mmol l^{-1}	Total F^-/ mmol l^{-1}	F^- adsorbed/ mmol/ kg
72	0.99	0.31	0.51	0.82	4.3
	1.96	0.84	0.45	1.3	17
	3.85	1.9	0.83	2.7	27
	5.66	3.0	1.7	4.7	25
	7.41	4.0	1.2	5.2	59
	9.09	5.2	0.36	5.6	96

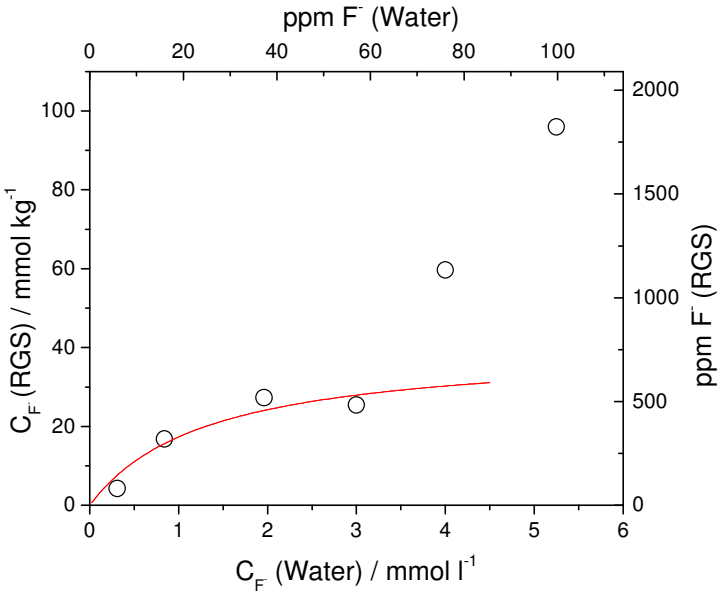

Figure 20. Adsorption isotherm obtained after 72 h contact time defluoridation.

The experimental data were fit with Langmuir isotherm model. As can be seen from Table 10 and Figure 20, the amount of fluoride adsorbed increases markedly for free fluoride concentration greater than 3.0 mmol l^{-1}. This may be attributed to the formation of stable aluminum-fluoride complexes at higher free fluoride concentrations which may be removed by being adsorbed on the soil. For example, for free fluoride concentration of 5.2 mmol l^{-1}, referring to Figure 4, AlF_3, AlF_4^- and AlF_5^{2-} are the main aluminum fluoride complexes that could be formed and they exist in the ratio 0.32: 0.50: 0.18, respectively. As can be seen from results of Table 10, the complexed fluoride concentration decreases with an increase in the free fluoride concentration. This may also indicate that some of the stable fluoride complexes formed at higher free fluoride concentrations are removed by adsorption on the soil.

Kau *et al.* [58], in their investigation to evaluate the potential effectiveness of kaolin clay liners, have also observed a similar phenomenon. They explained this observation on the basis of a site activation process which may occur during the fluoride removal. This is a process in which the initially adsorbed fluoride ions are supposed to create additional spaces for the other incoming fluoride ions. However, they have no experimental proof for their explanation as the subsequent X-ray analysis of the fluoride contaminated clay showed no detectable sign of any kaolin structural damage. Thus, it seems that their explanation was not correct.

The relationship among free, complexed and total fluoride for 72 h defluoridation is clearly shown in Figure 21 below.

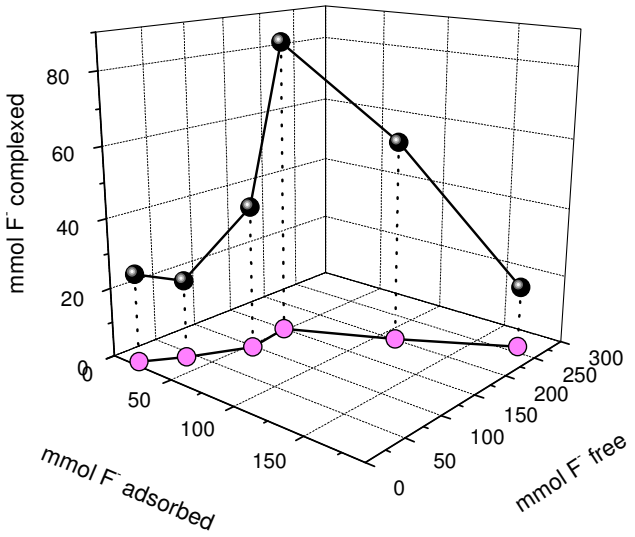

Figure 21. Three dimensional Langmuir isotherm for 72 h defluoridation of fluoride solutions.

As can be seen from Figure 21, the amount of fluoride complexed increases up to a certain point with an increase in free fluoride concentration as expected and passes through a maximum and then starts to decline with further increase in free fluoride concentration and as the amount of fluoride adsorbed increases. This may also imply that the stable aluminum fluoride complexes formed at higher concentrations might have been removed by adsorption on the soil.

4.2.7 Kinetics of fluoride removal

In most of the experiments the time dependence of the decrease in fluoride concentration has been studied. The results obtained can be used as a clue to elucidate the kinetics of fluoride

removal and draw conclusion about the mechanism of the defluoridation process. The way the experiments were performed has to be taken into consideration in order to avoid pitfall in the interpretation of the experimental results. Since the dry soil is added to a stirred solution of known fluoride concentration, the soil particles were suspended in the solution within the first few seconds of the experiments. In this process, the soil particles are moistened and water layers will be adsorbed at their surfaces and soluble constituents will dissolve. Simultaneously fluoride ions are brought in contact with the adsorption sites on the soil particle surface and fluoride adsorption onto the adsorption sites will occur creating a concentration gradient between bulk solution and surface of the "active" soil particle. Assuming that the rate of adsorption is fast compared to the diffusion of fluoride and with further assumption that the radial velocity of the heavier soil particles is less than that of the aqueous solution, the flux of fluoride to the surface of "active" soil particles is restricted by the concentration difference between the bulk and the particle surface and the thickness of the stagnant water layer adherent to the particle. Even this is a rather simple model for the real system; it may be used as a zero approximation to explain experimental results.

Fitting of the concentration-time curve with a theoretically reasonable function should yield some information about mechanism of fluoride removal. As expected from the above arguments about the diffusion control of the process, the best fits were obtained by utilizing non linear fitting with a second order exponential decay function. The experimental data was found to fit well with the following exponential decay function:

$$C(t) = C_o + C_1 \exp[-k_1 t] + C_2 \exp[-k_2 t] \qquad (22)$$

where $C(t)$ is concentration of fluoride at time, t; C_o is the concentration of fluoride at infinite time; C_1 and C_2 are constants having concentration units while k_1 and k_2 are rate constants. Values of these constants for the defluoridation of 1.96 mmol l^{-1} fluoride solutions by 2 g of untreated RGS and RGS fired at different temperatures for 4000 s are given in Table 11.

Table 11. Values of C_o, C_1, C_2, k_1 and k_2 obtained by fitting the experimental data to second order exponential decay function for defluoridation of 1.96 mmol l^{-1} fluoride solutions by untreated RGS and RGS fired at different temperatures.

Firing temperature/ ^oC	C_o	C_1	C_2	$k_1(s^{-1})$	$k_2(s^{-1})$
Untreated	8.0×10^{-4}	3.3×10^{-4}	1.1×10^{-3}	2.9×10^{-2}	4.7×10^{-4}
400	5.3×10^{-4}	6.4×10^{-4}	7.8×10^{-4}	1.8×10^{-2}	6.4×10^{-4}
500	3.2×10^{-4}	5.3×10^{-4}	1.2×10^{-3}	3.5×10^{-2}	7.7×10^{-4}
550	4.1×10^{-4}	1.7×10^{-3}	4.9×10^{-4}	2.8×10^{-2}	7.1×10^{-4}
600	4.8×10^{-4}	1.0×10^{-3}	4.4×10^{-4}	2.7×10^{-2}	7.6×10^{-4}
800	6.8×10^{-4}	6.4×10^{-4}	4.4×10^{-4}	1.0×10^{-2}	3.2×10^{-4}

The presence of two exponential terms, with two different rate constants, in eqn. (22) may indicate that the removal of fluoride by the soil involves two mechanisms: an initial rapid adsorption followed by slower uptake as can be seen from the two rate constants, k_1 and

k_2 respectively. Besides the adsorption at the outer surface of the adsorbent, the adsorbate molecules may diffuse into the interior of the adsorbent. The first rate constant, k_1, takes into account not only the removal of fluoride but also wetting of the soil particles and other processes occurring during the initial time of the experiment. Thus, it seems that the fluoride removal is mainly determined by the second process. The system under consideration is rather complex as a number of parameters, like area and mass of the soil particles, the velocity with which fluoride ion moves to the electrode surface, volume of the solution and stirring rate, have to be taken into consideration for complete quantitative descriptions. Thus, further work is required to develop a model, which takes into account all the above factors, and further theoretical explanations for this empirical finding.

5. CONCLUSION

The preliminary investigation of the electrochemical behavior of an aluminum electrode by cyclic voltammetry, impedance spectroscopy and potentiometry revealed that in low-fluoride solutions passivation of the aluminum anode will cause serious problems in its application in water defluoridation down to a limit of 1.5 ppm. Nevertheless at high fluoride concentrations the breakdown potential is shifted to negative values and electrolysis might be possible with a cell voltage not higher than 4 V. The growth rate of the oxide layer within the passive region of the aluminum electrode is assumed to be controlled by the diffusion of dissolved oxygen through the protecting layer. This conclusion was drawn from the results of impedance spectroscopy. The dissolution of the gibbsite layer occurs at the electrolyte/gibbsite interface. The dissolution rate in turn depends on the fluoride concentration in the electrolyte solution and will be enhanced at positive potentials due to electro-sorption of fluoride at the interface. If the dissolution becomes faster than the growth rate of the layer, the breakdown of the passivation is observed. The adsorption of fluoride ion at the gibbsite is also indicated by an increasing negative potential of the aluminum electrode with increasing fluoride concentration.

Comparison of the ability of the soils to remove fluoride with their mineral composition shows that there is a correlation between the stage of laterization characterized by an increasing aluminum oxide and ferric oxide content and fluoride removal. The speciation analysis of the fluoride remaining in the soil treated water reveals that about half of the fluoride is in the complexed form, most probably as aluminum fluoro complexes. This observation is insofar very important since it implies that in the course of fluoride removal a dissolution step is involved. On the other hand, aluminum fluoro complexes are suspected to

cause Alzheimer's disease as proved by recent studies on mice. This fact should not be overlooked when recommending lateritic soils as inexpensive defluoridation medium.

The adsorption isotherm of fluoride shows a sharp increase at higher initial concentration accompanied with a decrease in the concentration of complexed fluoride. This is an indication of a change in the mechanism of the fluoride removal. The adsorption of the aluminum tetrafluoro complex, which becomes at high fluoride concentration the dominating complex ion, might be a reasonable hypothesis.

Defluoridation experiments carried out with 2 g of the untreated RGS, ground clay pot, ground brick and RGS fired at 400 ^{o}C have revealed that the adsorbents removed 32, 36, 60 and 81% of fluoride from 50 ml of 18.8 ppm F^- within a contact time of 4000 s respectively. This result shows that firing an adsorbent at optimum temperature can significantly increase its defluoridating capacity. This result also implies that storage in clay pots, fired at relatively lower temperatures, may reduce the fluoride content of drinking water. Therefore, the traditional way of storing drinking water in clay pots should be encouraged in high fluoride areas as an alternative besides other defluoridation methods.

6. REFERENCES

1. Grim, J; Bessarobov, D.; Sanderson, R. *Desalination*, **1998**, 115, 285.

2. Staley, M.; Tatlow, J. C.; Sharpe, A.G. *Advances in Fluorine Chemistry*, Betterworths, London, **1961**, p. 35.

3. Parker, S. P. *Encyclopedia of Chemistry*, 2nd ed.; McGraw-Hill, Inc., New York, **1993**, p. 402.

4. Eagelson, M. *Concise Encyclopedia of Chemistry*, 2nd ed., Walter de Gruyter, Berlin, **1994**, p. 418.

5. Sheft, I. *Encyclopedia of Science and Technology*, Vol. 7, 7th ed., McGraw-Hill, New York, **1992**, p. 218.

6. American Dietary association, *J. Am. Diet. Assoc.*, **1994**, 94, 1428.

7. Klassen, C. D. *Cassaret and Doull's Toxicology: The Basic Science of Poison*, 6th ed., McGraw-Hill, New York, 2001, p. 4.

8. WHO, *Fluoride and Human Health*, Series 59, **1970**.

9. Padmasiri, J. P.; Dissanayake, C. B. *Intern. J. Environ. Health Res.*, **1995**, 5, 153.

10. Zevenbergen, C.; Reeuwijk, L. P. V.; Frapporti, G.; Louws, R. J.; Schuiling, R. D. *The Science of Total Environment*, **1996**,188, 225.

11. Weerassoria, R.; Wickramarathne, H. U. S.; Dharmagunawardhane, H. A. *Colloid and Surfaces A: Physicochemical and Energetic Aspects*, **1998**, 144, 267.

12. Goodman and Gilman, *The Pharmacological Bases of Therapeutics*, 6th ed., Macmillan, New York, **1980**, p. 1545.

13. Berhane, Y.; Demissie, B.; Zerihun, L.; Mekonnen, E.; Eshete, B. *Ethiop. J. Health Dev*. **2002**, 16 (2), 225.

14. WHO, *Fluorine and Fluorides*, World Health Organization, Geneva, **1984**.

15. WHO, *Fluorine and Fluorides*, Environmental Health Criteria 36, IPCS, International Program on Chemical Safety, World Health Organization, 1984.

16. Muller, W. J.; Heath, R. G. M.; Villet, M. H. *Water, SA*, **1998**, 24 (1), 219.

17. *Ethiopian Guidelines Specification for Drinking Water Quality*, Ministry of Water Resources, Addis Ababa, Ethiopia, **2002**.

18. Sujana, M. G.; Thakur, R. S.; Rao, S. B. *J. Colloid and Interface Sci.*, **1998**, 206, 94.

19. Haimanot, R. T.; Kloos, H. *J. Trop. Med. and Intern. Health*, **1999,** 4 (5), 355.

20. Haimanot, R. T.; Fekadu, A.; Bushra, B. *Trop. geogr. Med*. **1987**, 39, 209.

21. Gizaw, B. J. Afr. Earth Sci. **1996**, 22 (4), 391.

22. Chandra, S.; Thergaonkar, V. P.; Sharma, R. *Indian J. Publ. Health*, **1981**, 25, 47.

23. Teoita, S. P. S.; Teoita, M.; Sigh, R. K. *Fluoride*, **1981**, 14, 69.

24. Dunipace, A. J.; Brizendine, E. J.; Zhang, W. *J. Dental Res*., **1995**, 74, 358.

25. *Fluoride in Water*, Report by UNICEF, **2001**.

26. Hayatolla, I. H., *M. Sc. Thesis,* , Addiss Ababa University, Ethiopia, **1999**.

27. Essayas, A. *M. Sc. Thesis*, Addis Ababa University, Ethiopia, 2002.

28. Dahi, E.; Matlo, F.; Njou, B.; Bregnhj, H. *Report on 2nd WEDC Conference*, New Delhi, India, **1996**, p. 266.

29. Bruff, C. S. *Industrial and Engineering Chemistry*, **1934**, 26 (1), 69.

30. Bulusu, K. R.; Sundaresan, B. B. *J. Environ. Eng*.,1979, 60, 1.

31. Mameri, N.; Yeddou, A. R.; Lounci, H.; Belhouine, D.; Grib, H.; Bariou, B. Wat. Res., **1998**, 32 (5), 1604.

32. Ming, L.; Yi, S. R.; Hau, Z. J.; Lei, B. Y. W.; Ping, L.; Fuwa, K. C. *Fluoride*, **1983**, 20 (2), 54.

33. Walsh, F.; Millis, G. *Chem. Technol. Eur. J*, **1994**, 1, 13.

34. Li-Cheng, S. *Wat. Supply*, **1985**, 3, 177.

35. Zewge, F. *An investigation leading to the defluoridation of water in Ethiopia,* Report, **2001**, p. 11.

36. Commis, B. T. *Control of Eexcessive Fluoride Levels for Small Community Water Supplies with Particular Reference to Developing Countries:* an interim brief Report, Maidenhead, England, **1990**, personal communication.

37. Ouki, S.; Cheeseman, C.; Perry, R. *Environ. Sci. Technol*.,1993, 27, 1103.

38. Mjengra, H. J.; Matlo, F. W.; Mashauri, D. A.; Tjell, C. J. *2nd International Workshop on Fluorosis and Defluoridation of Water*, Dar es Salaam, Tanzania, **1997**, p. 101.

39. Bulusu, K. R.; Nawlakhe, G. W. *Indian J. Environ. Health*, **1990**, 32 (3), 197.

40. Bulusu, K. R., Nawlakhe, G. W. *Indian J. Environ. Health*, **1988**, 30 (3), 262.

41. Moges, G.; Zewge, F.; Socher, M. *J. Afr. Earth Sci*., **1996**, 21 (4), 479.

42. Bjorvatn, K.; Reimann, C.; Haimanot, T. R.; Melaku, Z. *High Fluoride in Drinking Water; a Health Problem in Ethiopian Rift Valley*, personal communication.

43. Lubkowska, A.; Zyluk, B.; Chlubek, D. *Fluoride*, **2002**, 35 (2), 73.

44. MacDougall, B.; Graham, M. J. *J. Electrochem. Soc*., **1987**, 134 (5), 104.

45. Bokris, J. O. M.; Khan, S. U. M. *Surface Electrochemistry: A Molecular Level Approach*, Plnum Press, New York, **1993**, p. 772.

46. Sparks, L. D. *Environmental Chemistry*, Academic press, New York, **1995**, p. 203.

47. Wade, K.; Banister, J. A. *Comprehensive Inorganic Chemistry*, 1st ed., Pergamonn Press, Oxford, **1973**, p. 993.

48. Goldich, S. S.; *Encyclopedia of Science and Technology*, Vol. 9, 7th ed., McGraw-Hill Inc., New York, **1992**, p. 630.

49. Norton, B. T.; Esposito, J. J. *The New Encyclopedia of Britannica*, Vol. 7, 15th ed., Encyclopedia Britannica, Inc., Chicago, **1995**, p. 179.

50. Selley, C. R. *An Introduction to Sedimentology*, Academic Press, London, **1976**, p. 61.

51. Bailey, P.L, *Analysis with Ion- selective Electrodes*, 3rd ed., Heiden, London, **1980**, p. 196.

52. Koryata, J. *Ion-selective Electrode*, Cambridge University Press, London, **1975**, p. 102.

53. Appleby, A. J. *Comprehensive Treatise of Electrochemistry*, Vol. 7, Plumn Press, New York, **1983**, p. 230.

54. Boukamp, B. A. *Equivalent Circuit: The Computer Assisted Electrochemical ac Immittance Analysis System for IMBM-PC Computers and Compatibles*, Users Manual 2nd ed., University of Twente, **1989**.

55. Rigbon, A. *Complexation in Analytical Chemistry*, Interscience, New York, **1963**.

56. Grim, R. E. *Clay Mineralogy*, 2nd ed., McGraw-Hill, Inc., New York, **1968**, p. 298.

57. Choi, W. W., Chen, Y. K. *JAWWA*, **1979**, 71, 562.

58. Kau, P. M. H.; Binning, P. J.; Hitchock, P. W.; Smith, D. W. *J. Contam. Hydrology*, **1999**, 36, 131.